INTERNATIONAL ATOMIC ENERGY AGENCY
UNITED NATIONS EDUCATIONAL, SCIENTIFIC AND CULTURAL ORGANIZATION

INTERNATIONAL CENTRE FOR THEORETICAL PHYSICS
34100 TRIESTE (ITALY) - P.O.B. 586 - MIRAMARE - STRADA COSTIERA 11 - TELEPHONE: 2240-1
CABLE: CENTRATOM - TELEX 460392-I

H4.SMR/381-13

COLLEGE ON ATOMIC AND MOLECULAR PHYSICS:
PHOTON ASSISTED COLLISIONS IN ATOMS AND MOLECULES

(30 January - 24 February 1989)

- ASSOCIATIVE IONIZATION
- MOLECULE FORMATION
- PROSPECTS OF ENERGY POOLING COLLISIONS

M. ALLEGRINI

Dipartimento di Fisica
Università di Pisa
Pisa

LECTURE III

- ASSOCIATIVE IONIZATION
- MOLECULE FORMATION
- PROSPECTS OF ENERGY POOLING COLLISIONS

ASSOCIATIVE IONIZATION

$$A^* + A^* \xrightarrow{k_{AI}, \sigma_{AI}} A_2^+ + e^-$$

BEST KNOWN of the 3 PROCESSES

Experiments in cells $T \approx 500-650\ ^\circ K$

Experiments in beams wide range of T

Measurements of average σ_{AI} and also dependence upon

1. POLARIZATION
2. VELOCITY

of colliding atoms

① Morgenstern et al.
Rothe et al.
Hertel et al.
Weiner et al.

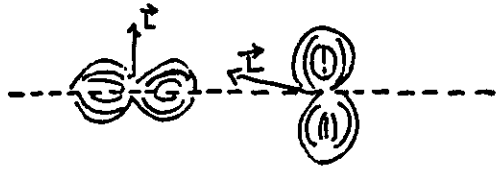

m_L $m_L=0$ $m_L=1$ $m_L=-1$

σ_{11}
σ_{10}
σ_{1-1}
σ_{00}

② Weiner - Phillips NBS et al.

$\sigma_{AI}(20\ ^\circ K) \approx 10^{-16}\ cm^2$

$\sigma_{AI}(0.75\ m^\circ K) = 8.6 \times 10^{-14}\ cm^2$

≈ 3 orders of magnitude bigger

[Weiner lectures]

LOW TEMPERATURE – LOW ENERGY REGIME

(Gould et al. PHYS. REV. LETT 60 788 (1988))

i) COLLISIONS CAN BE HIGHLY NON CLASSICAL:
$\lambda_{de\ Broglie}$ of COLLIDING PARTICLES > RANGE of INTERACTION POTENTIALS

ii) ONLY A SMALL NUMBER of PARTIAL WAVES CONTRIBUTE TO σ_{AI}

iii) COLLISION DYNAMICS CAN BE DOMINATED BY WEAKLY ATTRACTIVE LONG-RANGE POTENTIALS, UNIMPORTANT AT HIGH COLLISION ENERGIES

⇝ σ_{AI} so big may limit atom density achievable in laser-cooling, laser-trapping experiments.

(Vigué Phys. Rev. A34 4476 (1986))
(P. JULIEN theory)

ION DETECTION : several method

EUECTRON DETECTION : spettrometry (difficult at low energies)

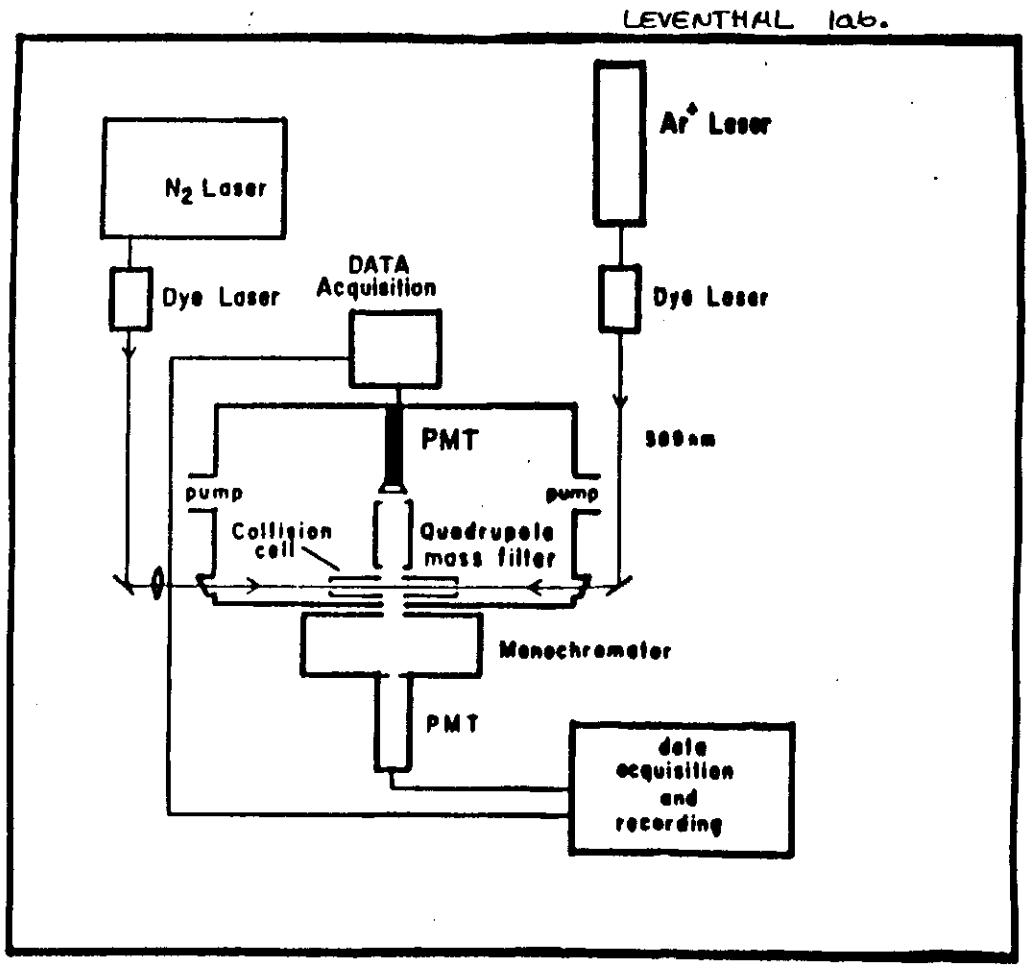

FIG. 1. Schematic diagram of the apparatus used in the present study.

2 MODES OF EXCITATION < cw / pulsed

2 MODES OF OPERATION :

i) λ_L fixed at atomic transition ⟶ MASS SCAN

ii) Quadrupole fixed at one ion mass ⟶ λ_L SCAN

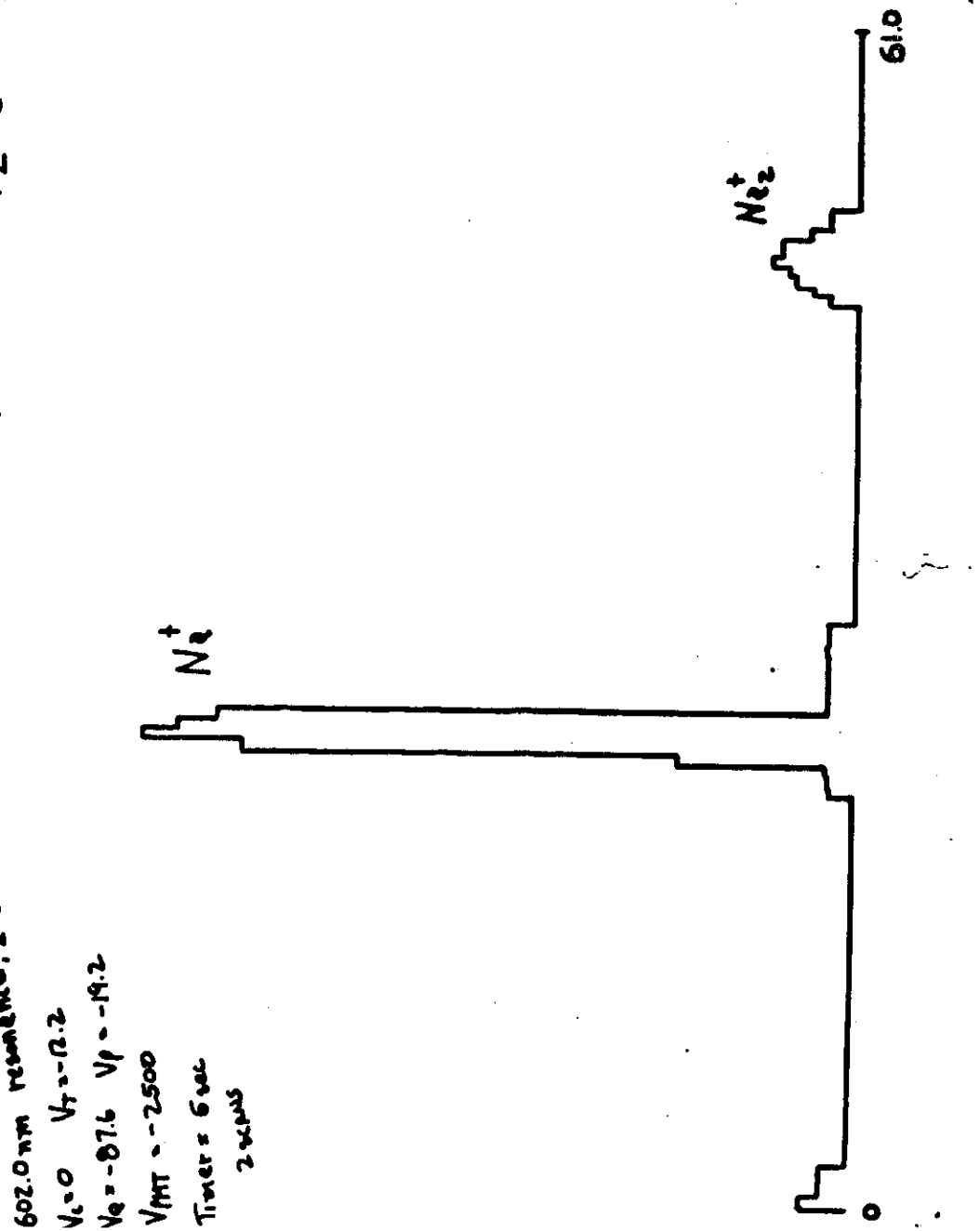

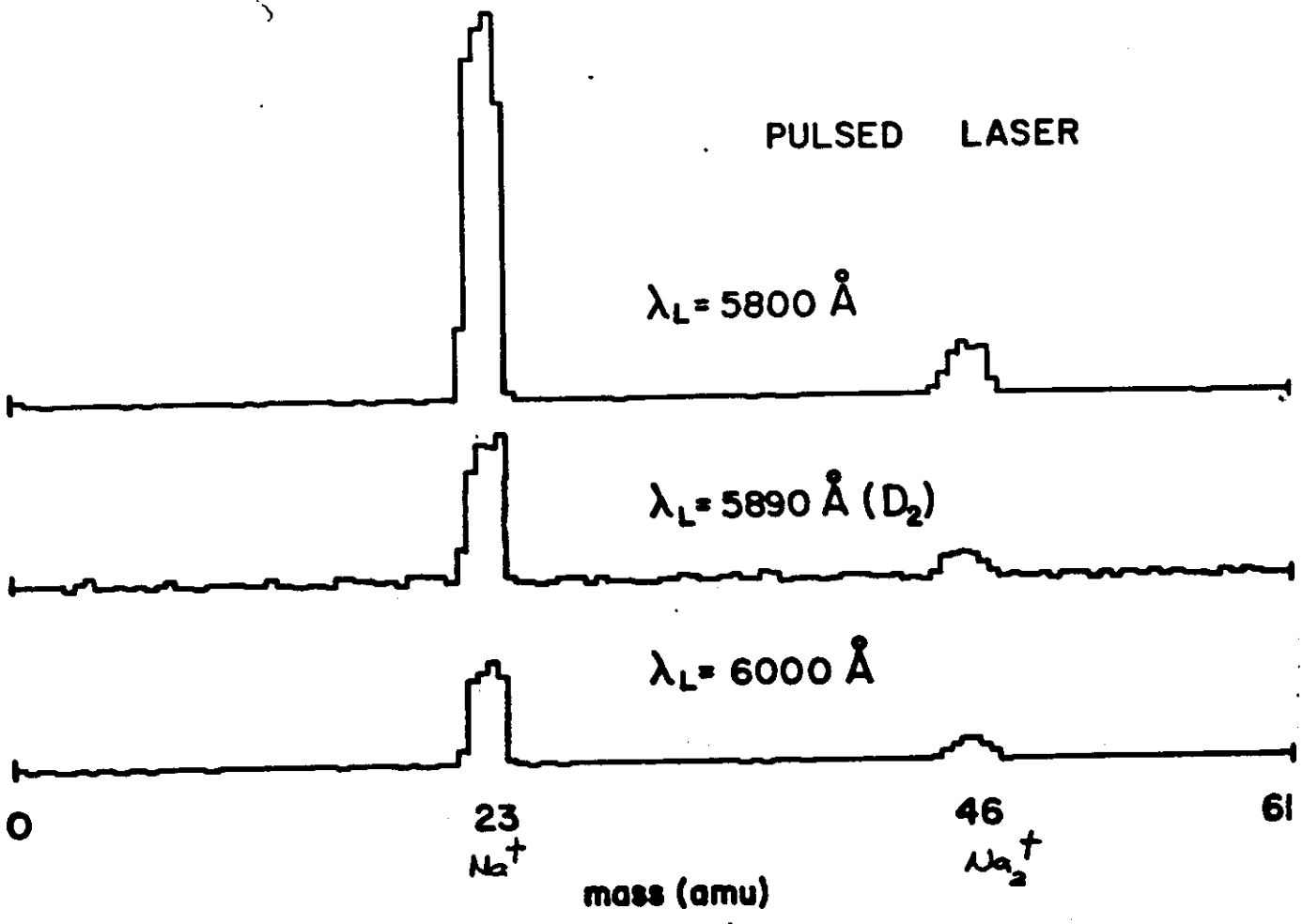
PULSED LASER
λ_L = 5800 Å
λ_L = 5890 Å (D_2)
λ_L = 6000 Å
0
23
Na^+
46
Na_2^+
61
mass (amu)

10/8/82

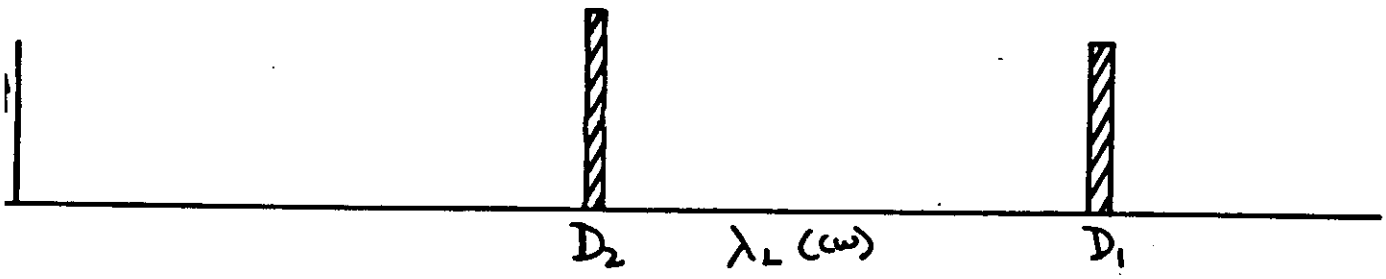
D_2
λ_L (ω)
D_1

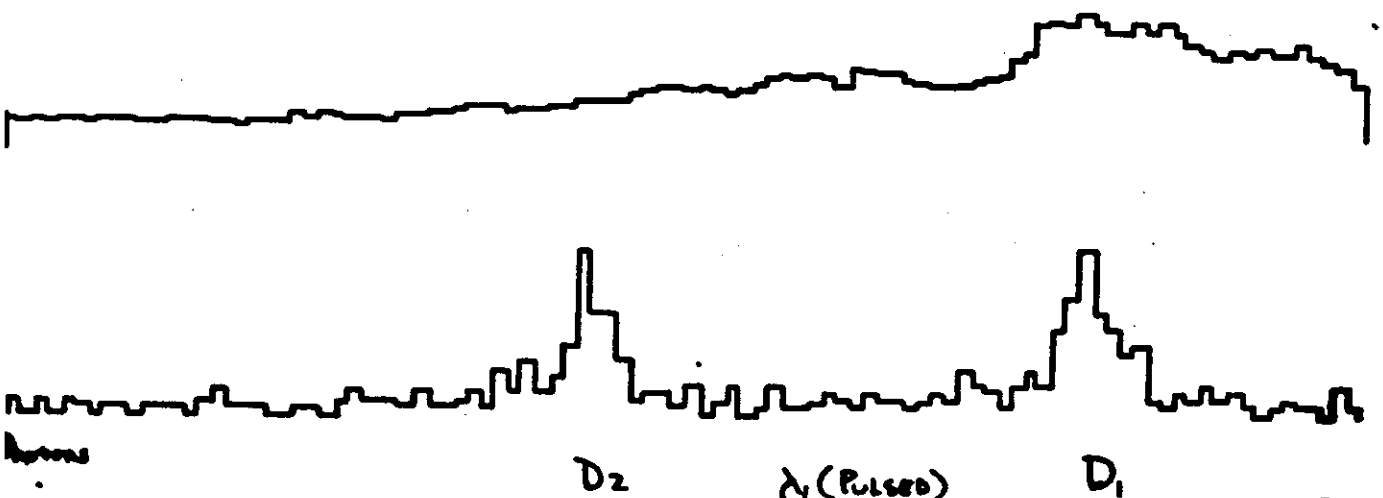
D_2
λ_L (Pulsed)
D_1

CARRÉ et al. (SACLAY - ORSAY - NBS - STONY BROOK COLLABORATION)

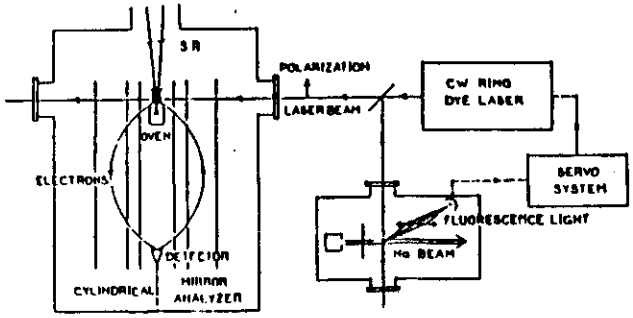

Fig. 1. Experimental apparatus. The laser was locked to the $3\,^2S_{1/2}(F=2) \rightarrow 3\,^2P_{3/2}(F=3)$ transition by monitoring the fluorescence of an auxiliary sodium beam.

- Associative ionization of excited atoms and superelastic collisions between electrons and excited atoms : Peak labelled a at energy 0.05 ± 0.03 eV corresponds to electrons produced by associative ionization in the collision of two Na(3p) atoms :

(1) $\boxed{Na(3p) + Na(3p)} + W \rightarrow \boxed{Na_2^+ (^2\Sigma_g(v)) + e\,(E_e)}$

where W is the kinetic energy of the colliding atoms and v a particular vibrational level in which Na_2^+ is formed. The electrons produced in (1) may undergo p = 1, 2, 3 subsequent superelastic collisions with Na(3p) atoms, each of which boosts their energy by 2.1 eV :

(2) $Na(3p) + e\,(E_e) \rightarrow Na(3s) + e\,(E_e + 2.1\ eV)$

The corresponding peaks a + p primes are observed in spectra a) and b). For a pulsed laser excitation of the 3s-3p transition, structures similar to peaks a and a' are observed as shown in the spectrum in Fig. 2.

- Penning ionization of excited atoms :
In spectrum a) in Fig. 1, peaks b, c, d, and e correspond to the electrons produced by Penning ionization in the collision of Na(nl) and Na(3p) atoms with, respectively, nl = 3d, 4p, 5s and 4d/4f :

(3) $\boxed{Na(nl) + Na(3p)} \rightarrow \boxed{Na^+ + Na(3s) + e\,(E_{3p} - E_b(nl))}$

where $E_b(nl)$ is the binding energy of the electron in the nl state. The primary electrons which have been superelastically heated in process (2) are also observed after p = 1, 2 superelastic collisions. These electrons appear on a larger scale (for p = 1 SEC) and with a better resolution in Fig. 3 at temperature T_0 = 520 K.

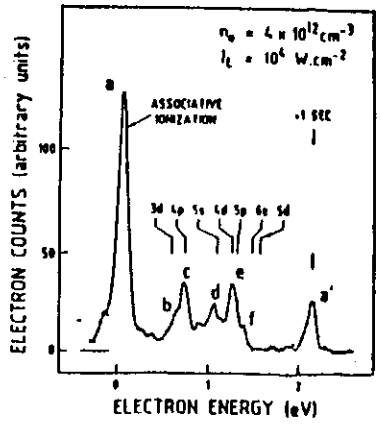

FIGURE 2
Electron energy spectrum measured between 0 and 2.5 eV in Na vapor ($T_0 \sim 550$ K) excited with a pulsed laser tuned to the $3S_{1/2} \rightarrow 3P_{3/2}$ transition. The labelling of the peaks is the same as in spectrum a) in Fig. 1. However notice that peak b, c, d and f are mainly produced by photoionization of Na(nl).

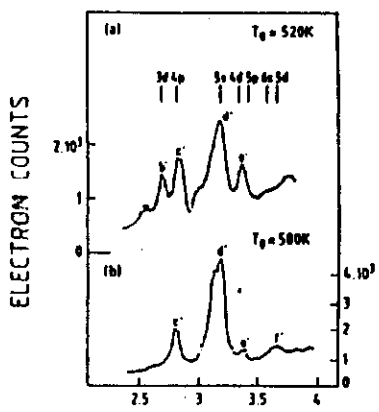

Fig. 4. Electron energy spectra produced by Penning ioni (ion of Na(nl) atoms followed by one superelastic collisi in laser-excited Na vapor.

The nl = 5s and 4d/4f states are populated in the energy pooling collisions of two Na(3p) atoms :

(4) $\boxed{Na(3p) + Na(3p)}^{**} + \Delta w \rightarrow \boxed{Na(nl) + Na(3s)}^{*}$

where Δw is the energy defect of the reaction. Process (4) was first observed from fluorescence measurements by M. Allegrini et al. / 18 / ; the role of this process in the ionization is now clearly demonstrated from the electron energy spectra. Instead of a direct population by process (4), the 3d and 4p states are populated by radiative decay from upper-lying 5s and 4d/4f states.

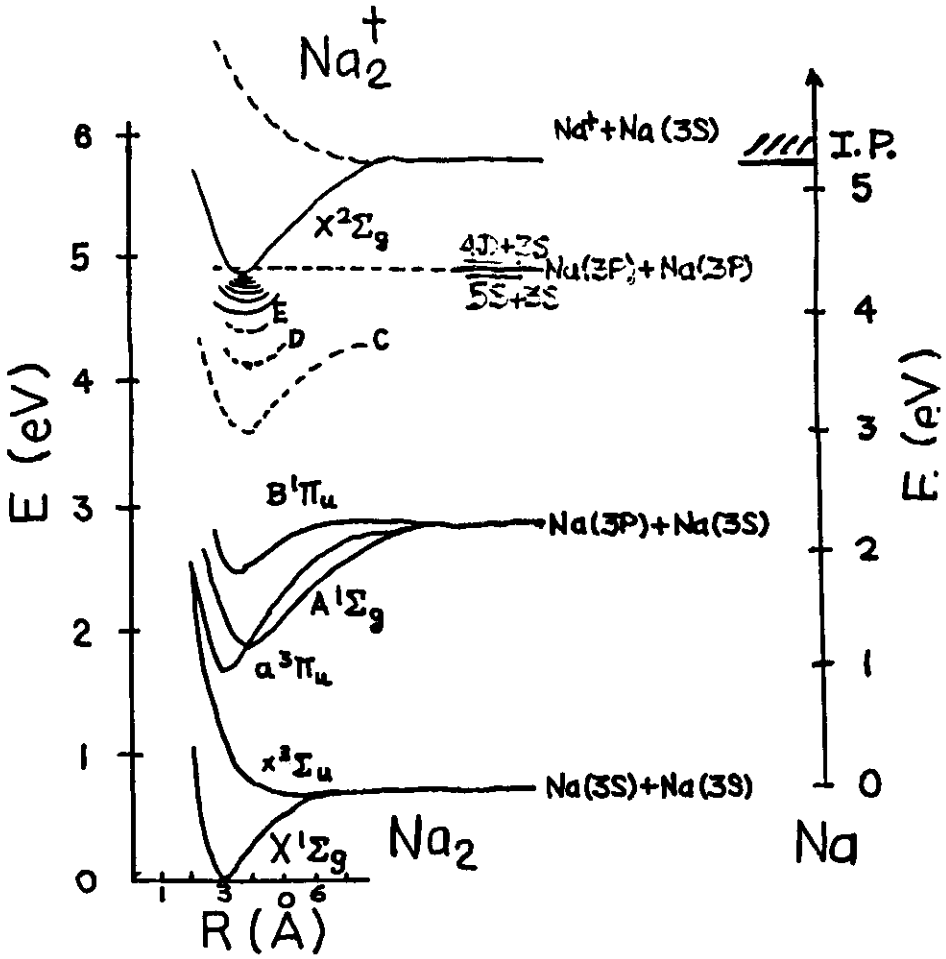

LUCATORTO and McILRATH Phys. Rev. Lett. 37, 428

NEARLY COMPLETE IONIZATION IN A 10-cm COLUMN of Na.

pulsed LASER → Na VAPOR
D-line
$W_L \simeq 1\ MW/cm^2$
$\Delta t \simeq 1\ \mu sec$
$\sim 10^{16}\ cm^{-3}$

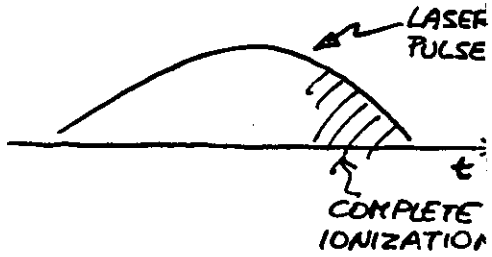

MECHANISM PROPOSED :

Associative Ionization $Na^*(3P) + Na^*(3P) \rightarrow Na_2^+ + e$

e SEED ELECTRON, low energy $\simeq$ few kT

Superelastic Collisions $e + Na^*(3P) \rightarrow e(FAST) + Na(3S)$

$e(FAST) + Na^*(3P) \rightarrow Na^+ + 2e$

MEASURES and CARDINAL Phys. Rev. A 23, 804 (198

EXCITED MOLECULE FORMATION

$$A^* + A^* \xrightarrow{K_{NP}, \sigma_{NP}} A^{**}$$

LESS STUDIED of the 3 PROCESSES

A^{**} can be singlet or triplet state

⇒ spectroscopy of triplet states (diffuse bands)

- excimer configuration: population inversion → tunable laser sources ?

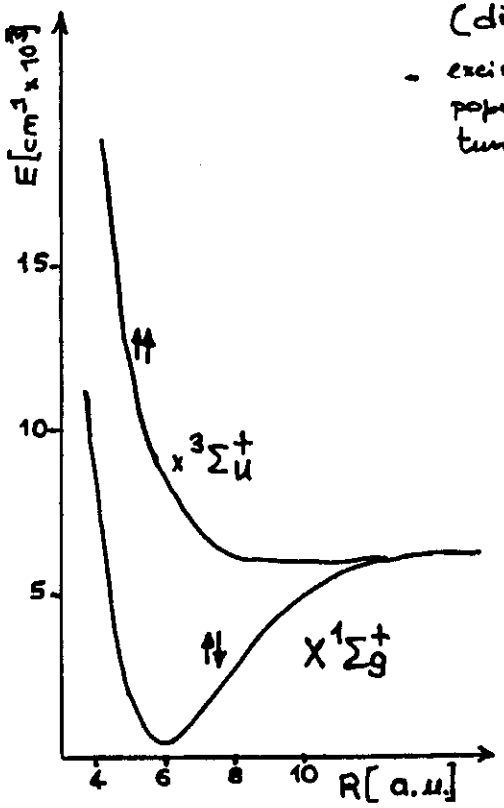

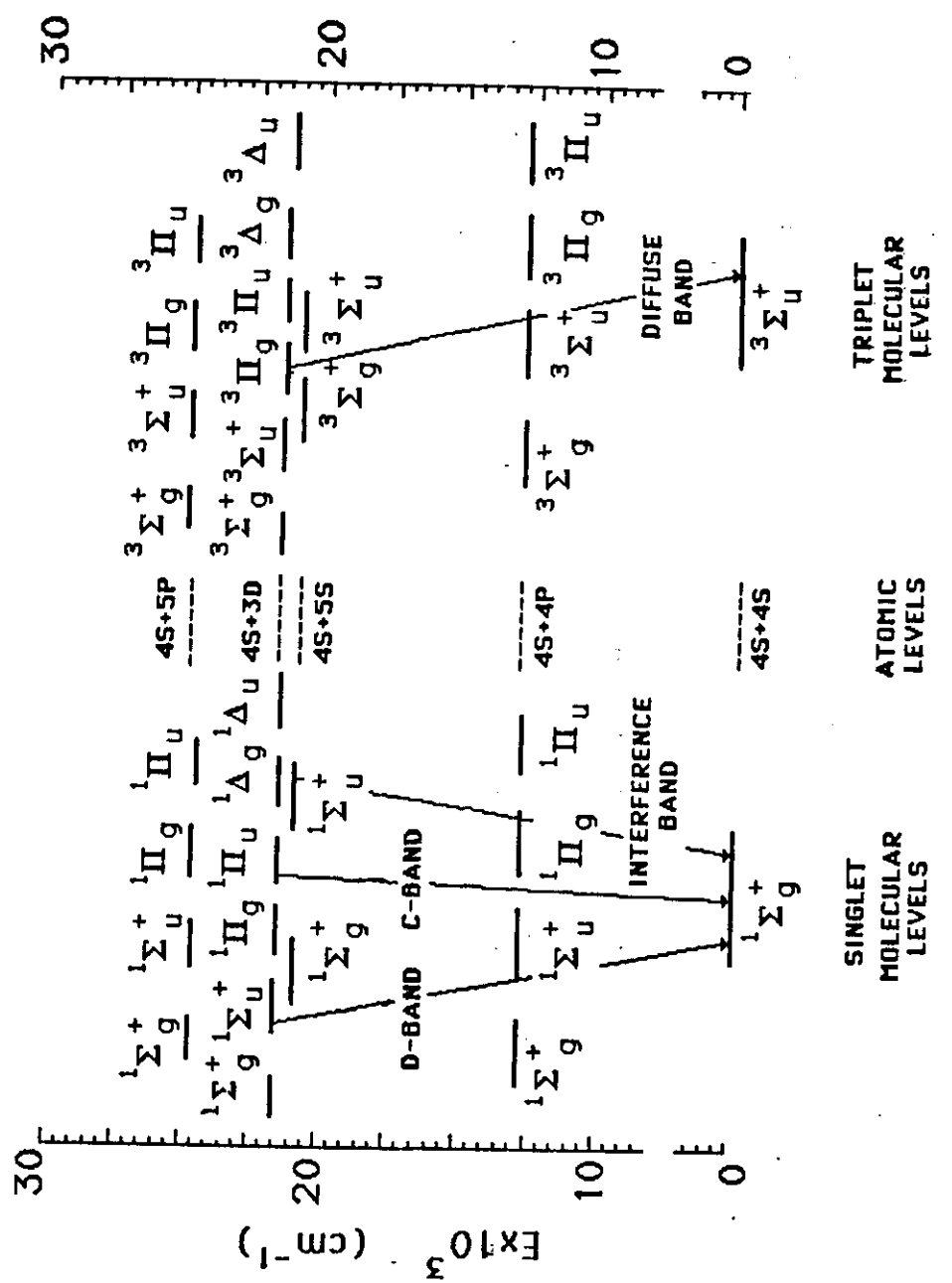

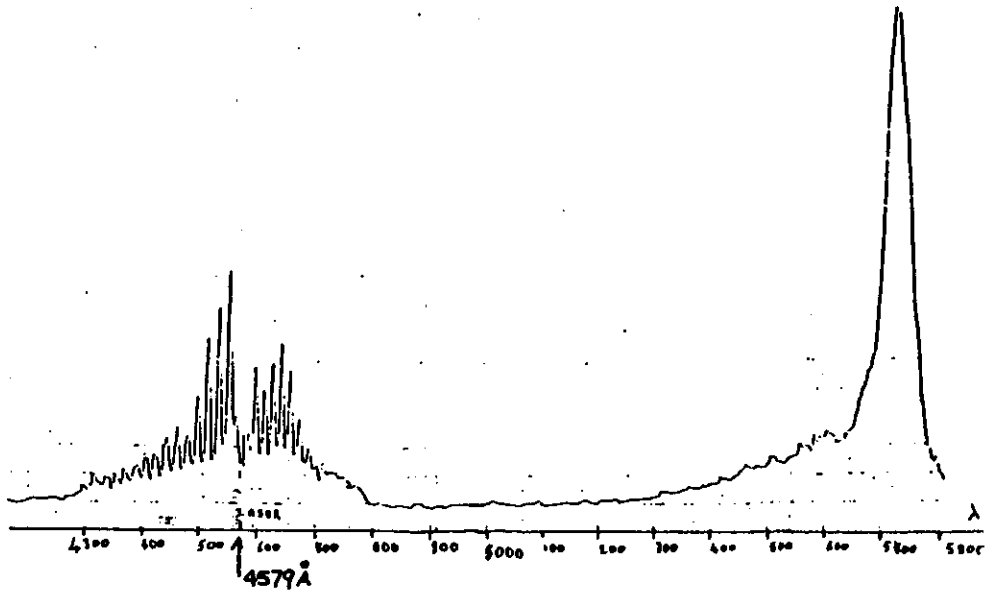

Fig. 3-6: spettro in fluorescenza del K_2 a 600°C.

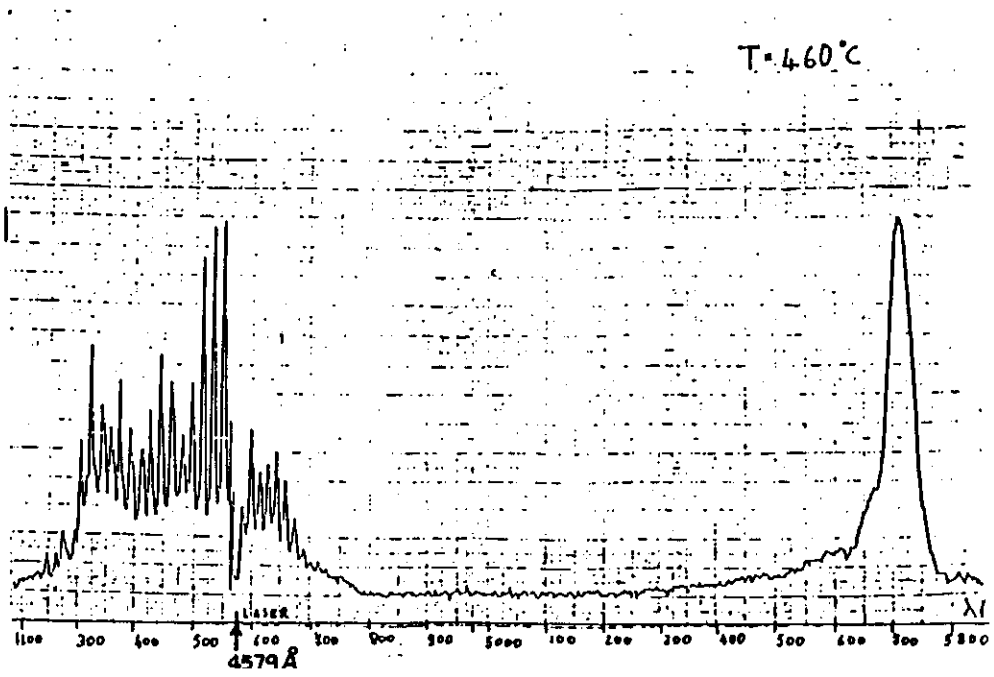

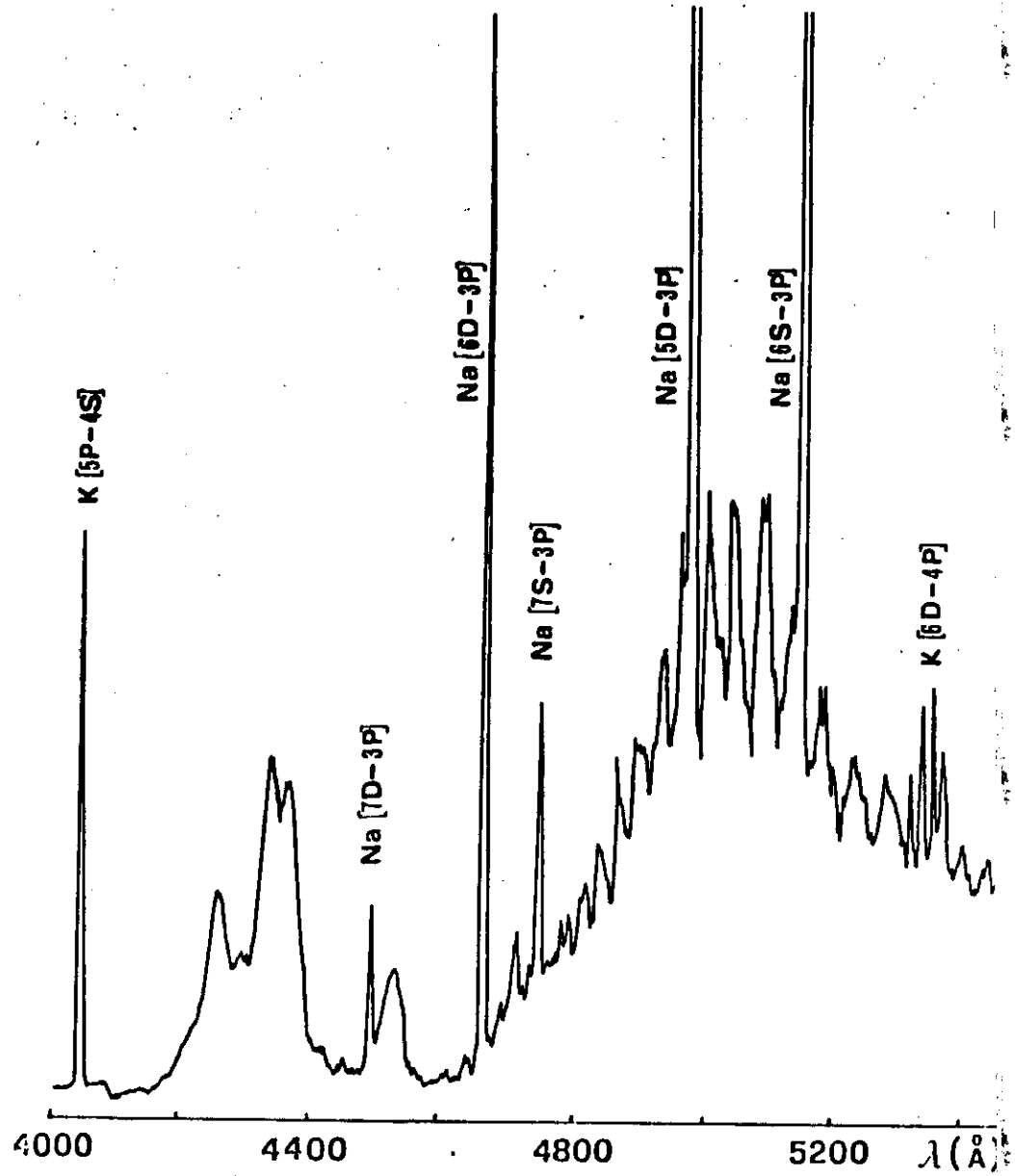

LIVELLI ATOMICI CON $\Delta E > 10kT$

BANDE MOLECOLARI $A^1\Sigma_u^+ \rightarrow X^1\Sigma_g^+$

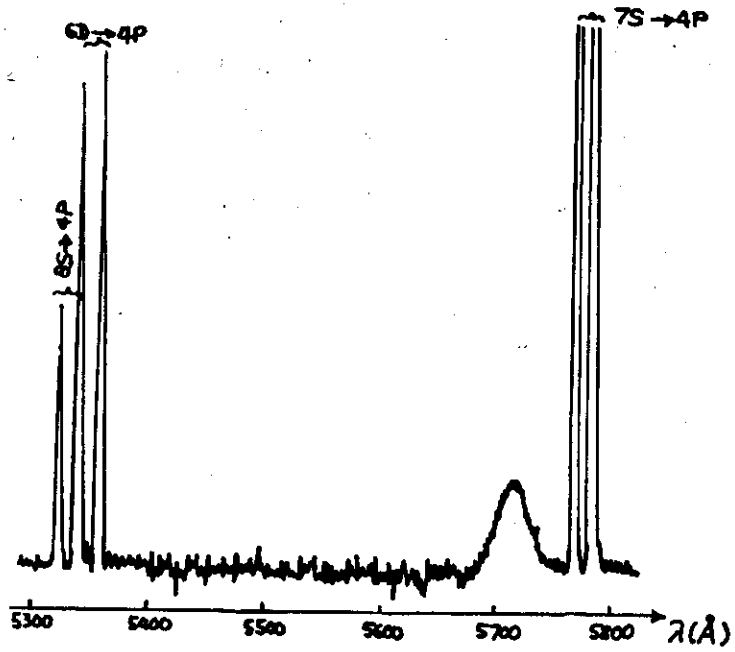

STUDIES of DIFFUSE BANDS in ALKALI DIMERS : W. STWALLEY and coll.
G. PICHLER " "

PROSPECTS of ENERGY POOLING COLLISIONS

1. A^*/A^* COLLISIONS : theory
   low-temperature
   molecule

2. COLLISIONS involving highly excited atoms (RYDBERG ATOMS)

   i) $A^{**} + A \longrightarrow A^+ + A + e^-$ ION FORMATION (PENNING IONIZATION)

   $\longrightarrow A^+ + A^-$ ION-PAIR FORMATION

   $\longrightarrow A_2^+ + e^-$ ASSOCIATIVE IONIZATION

   ii) $A^{**} + A^{**} \longrightarrow A^+ + A + e^-$

   $\longrightarrow A^+ + A^-$

VERY HIGH CROSS-SECTIONS (RYDBERG ATOMS are "large")
but ...

PHOTOIONIZATION from BLACK-BODY RADIATION

$$A^{**} + \hbar\omega_{bb} \longrightarrow A^+ + e^-$$

[LEVENTHAL lectures]

quantity	asymptotic n behavior	n = 1	n = 30
orbital radius	n^2	0.53 Å	477 Å
cross sectional area	n^4	0.9 $Å^2$	7E5 $Å^2$
orbital velocity	n^{-1}	2.2E8 cm/sec	7.3E6 cm/sec
ionization potential	n^{-2}	5.1 eV(Na)	.015 eV
Energy level separation	n^{-3}	2.1 eV(Na)	.001 eV
radiative lifetime	n^3	16 nsec	3E4 nsec

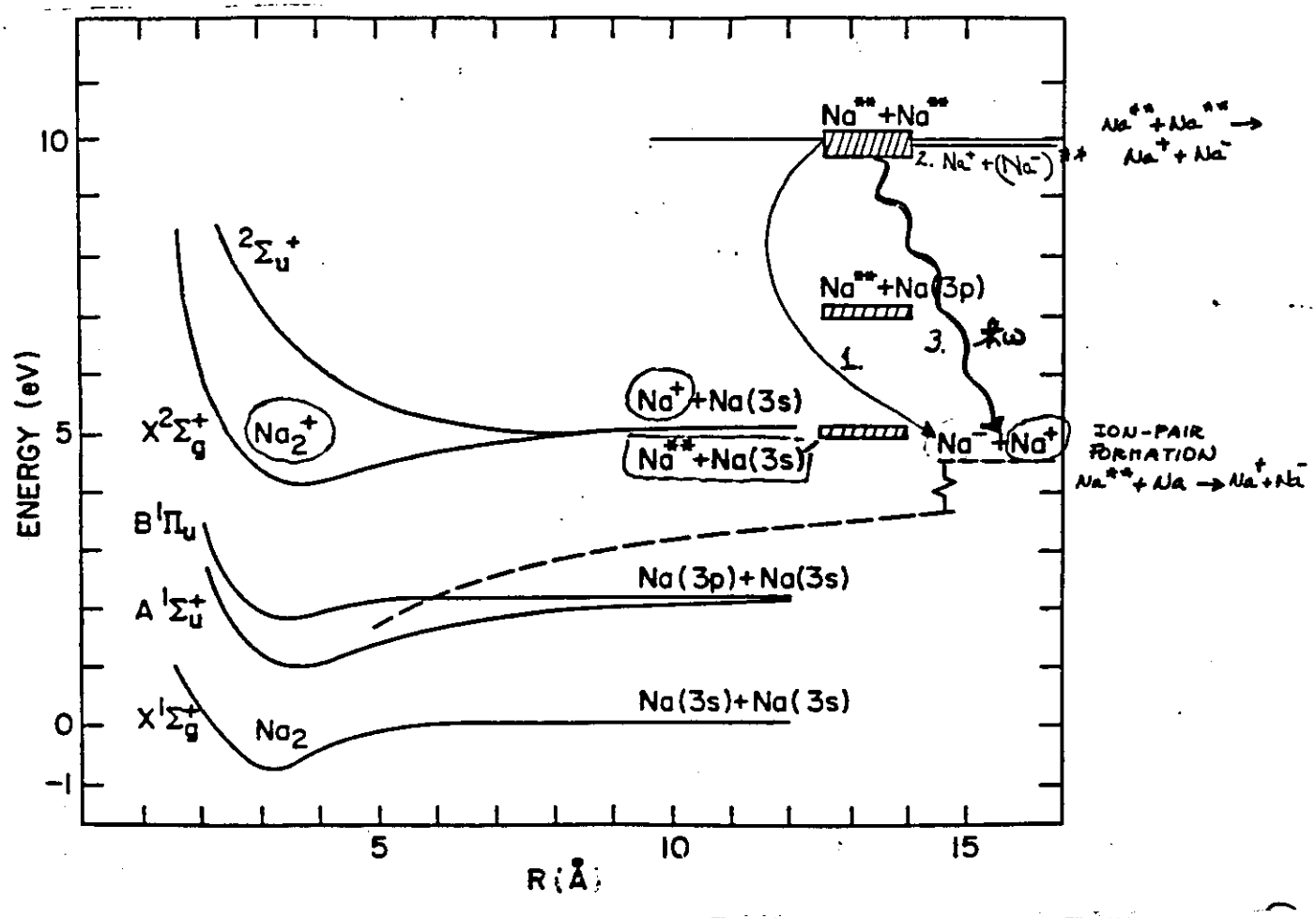

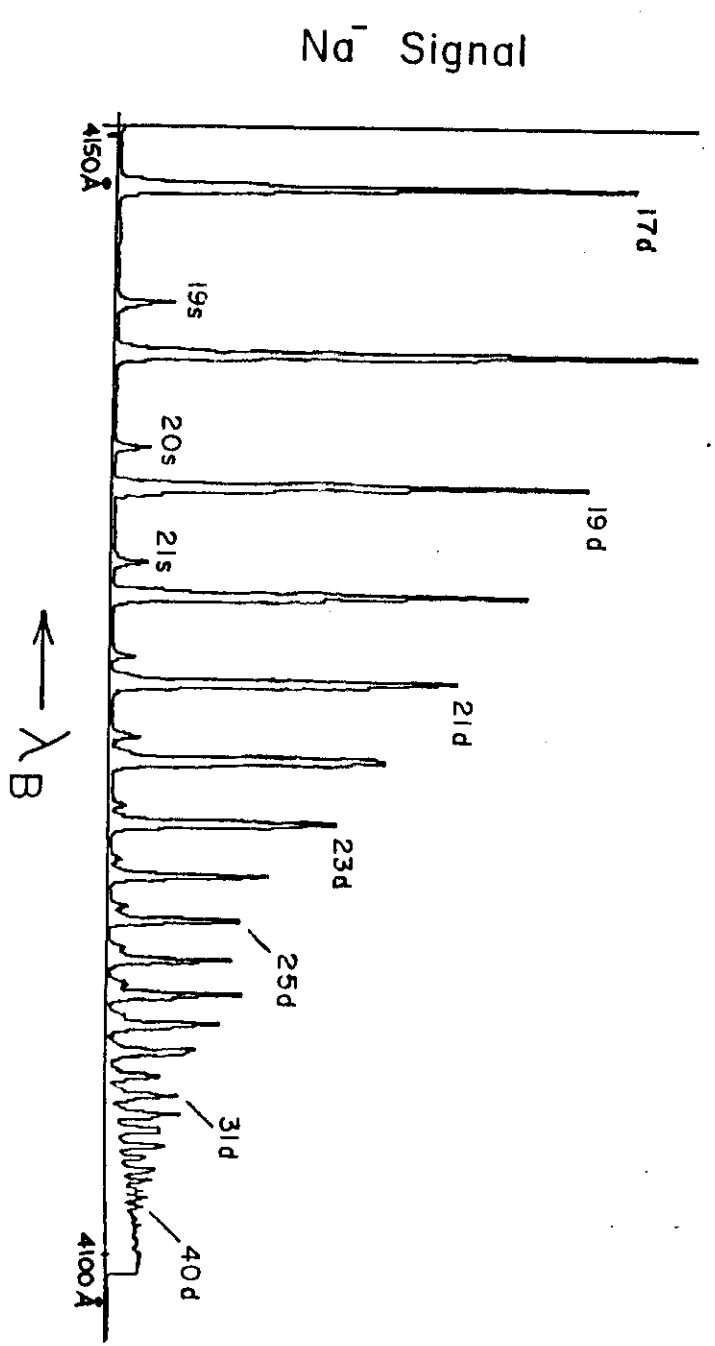
Na⁻ Signal
4150Å
17d
19s
20s
19d
21s
21d
23d
25d
31d
40d
4100Å
λB

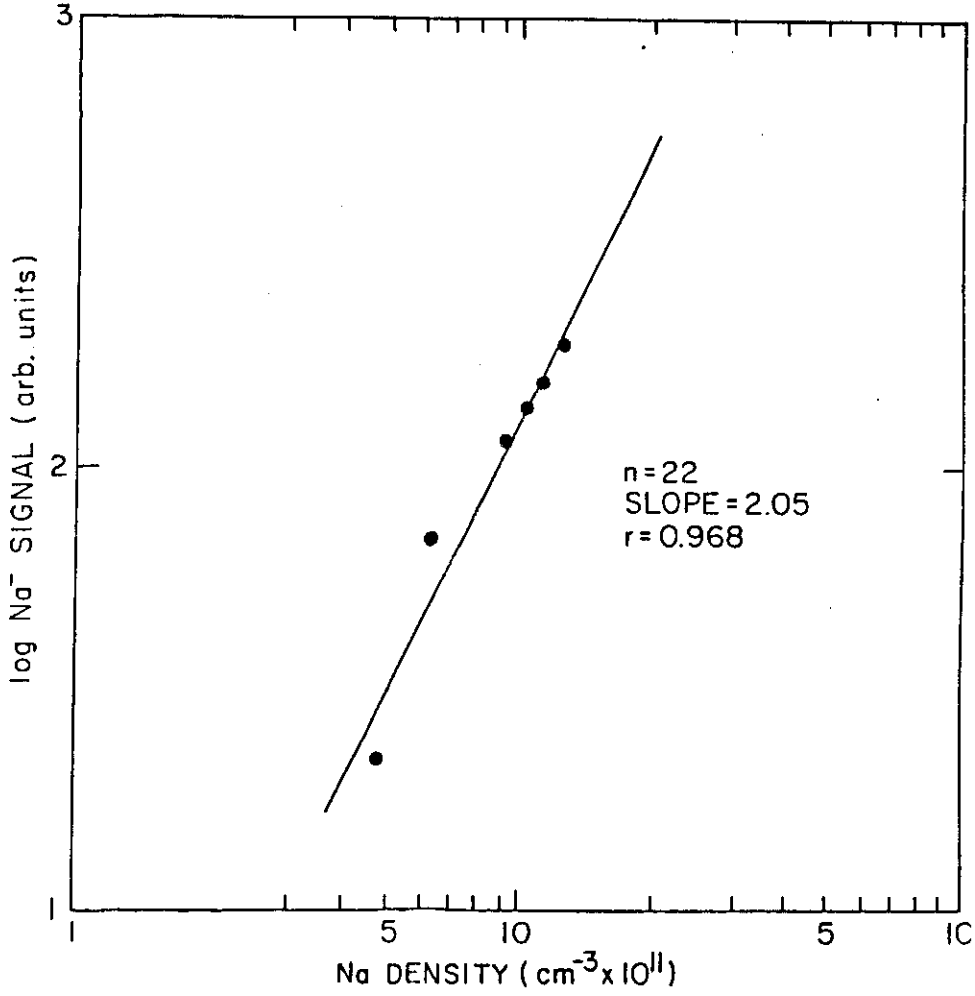
log Na⁻ SIGNAL (arb. units)
3
2
1
n = 22
SLOPE = 2.05
r = 0.968
1
5
10
5
10
Na DENSITY (cm⁻³ x 10¹¹)

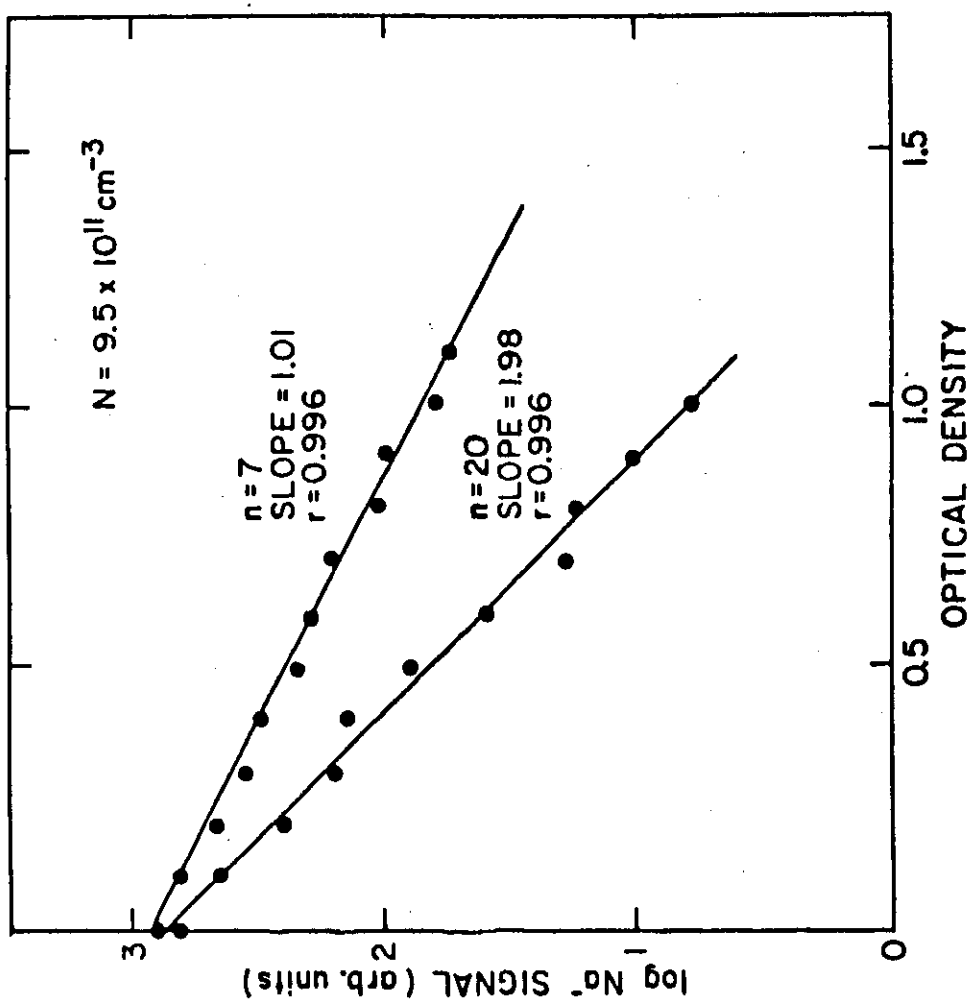

POSSIBLE MECHANISMS FOR Na^- FORMATION IN Na^{**}/Na^{**} COLLISIONS

1. $Na^{**} + Na^{**} \longrightarrow Na^+ + Na^- + KE(\approx 5.5\ eV)$

2. Formation of a "planetary negative ion" with electron configuration $(1s)^2\,(2s)^2\,(2p)^6\,nln'l'$

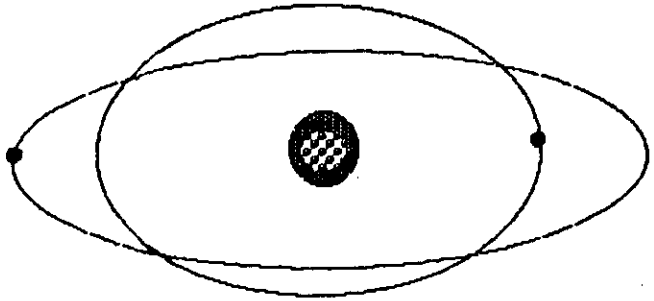

3. Radiative attachment in an e/Na^{**} - like collision.

$$Na^{**} + Na^{**} \longrightarrow Na^+ + Na^- + \hbar\omega\ (\approx 5.5\ eV)$$

1. REACTION IS EXOTHERMIC BY ~ 5.5 eV
$(Na^+)^*$ IS ENERGETICALLY PRECLUDED
$(Na^-)^*$ HAVE NEVER BEEN OBSERVED
$\Rightarrow$ $Na^{**} + Na^{**}$ SYSTEM SHOULD EVOLVE FROM THE ENTRANCE CHANNEL at ~10eV TO $Na^+ + Na^-$ EXIT CHANNEL VIA A SERIES OF CROSSINGS WITH POTENTIAL CURVES IN THE ~5 – 10 eV RANGE.
$\approx\Rightarrow$ SHARING OF ~5.5 eV AS KINETIC ENERGY OF THE $Na^+ + Na^-$ PRODUCTS IS VERY UNLIKELY

2. DOUBLY EXCITED Na^- WITH OUTER ELECTRONS IN CORRELATED RYDBERG ORBITS.
THIS PROVIDE AN EXIT CHANNEL CLOSE TO THE ENTRANCE CHANNEL
$\approx\Rightarrow$ SUCH STATE WOULD BE IMBEDDED IN THE $Na + e$ CONTINUUM
WOULD HAVE AN AUTODETACHMENT LIFETIME IN EXCESS OF ~ 1 μsec TO BE OBSERVED IN OUR APPARATUS

HIGHLY SPECULATIVE

3. SIMILAR TO RADIATIVE ATTACHMENT $\rightsquigarrow$
AFFINITY SPECTRUM. (SOLAR SPECTRUM)
INVERSE PROCESS (PHOTODETACHMENT ACCOMPANIED BY NEUTRAL EXCITATION)
HAS BEEN OBSERVED IN THE LABORATORY

$\approx\Rightarrow$ WE SEARCHED FOR 5.5 eV PHOTONS
– USE 2250 Å FILTER ($\Delta\lambda = 100$ Å), 4 O.D.
SMALL SIGNAL MAY BE MASKED BY FLUORESCENCE FROM PRINCIPAL SERIES (limit ~ 2400 Å)

EXPECTED NUMBER OF PHOTONS
~50 per laser pulse $\Rightarrow$
REPLACEMENT OF FILTER WITH MONOCHROMATOR GAVE NO SIGNAL AT ~2250 Å, WHILE PRINCIPAL-SERIES EMISSION WAS THERE.

POSSIBLE MECHANISM

(c)

- AT HIGH n σ^- (Na_2^+ FORMATION) IS KNOWN

- $Q^- \propto k \left[N_0^{**}\right]^2 V(\tau/2)\, K^-$

  - Q^-: Na^- produced per laser pulse
  - k: collection efficiency
  - N_0^{**}: initial concentration of Rydberg atoms
  - $V(\tau/2)$: effective lifetime of Na^{**}
  - K^-: rate constant

- Q^+ Na_2^+ produced per laser pulse

- $\frac{Q^-}{Q^+} = \frac{1}{2} \frac{N_0^{**}}{N} \frac{k^-}{k^+} \Rightarrow$ $K^- \approx 10^{-7}\ cm^3\ sec^{-1}$, $\sigma^- \approx 10^4\ Å^2$ $n=27$

- σ^- from time of flight measurements was within a factor of 4

IMPORTANCE :

- INTRINSIC PROPERTIES of ATOMS
- SOLAR PHYSICS (radiative attachment of electrons to H atom in the photosphere strongly influence the solar spectrum)
- ASTROPHYSICS
- PLASMA PHYSICS (generation of intense negative ion beams required for neutral beam heating of a plasma)

ENERGY-POOLING PROCESSES IN LASER-EXCITED ALKALI VAPORS : AN UPDATE ON EXPERIMENTS

M. Allegrini, C. Gabbanini and L. Moi

Istituto di Fisica Atomica e Molecolare del C.N.R., Via del Giardino, 7, Pisa, Italy

Résumé - Les processus d''energy pooling' dans les vapeurs atomiques alcalines excitées par laser sont passés en revue. On présente en particulier les résultats les plus récents obtenus pour le sodium.

Abstract - We present a short review of energy pooling experiments in laser excited alkali vapors, for low atom density and low radiation intensity. Special emphasis is devoted to the most recent results obtained in sodium vapor.

I - INTRODUCTION

Laser excitation of dense vapors produces a large variety of atomic and molecular processes /1/, that are not easily separated in the experiments. Thus these kinds of experiments offer on the one hand a very rich and interesting way of studying atom-atom and atom-e.m. field interactions, but on the other hand they suffer of the difficulties associated with the correct interpretation of the observed phenomena. To simplify this matter it is convenient to select in the experiment the proper values of the parameters that may determine the dominant effect, namely the laser power density, the atom and molecule densities in the vapor and, last but not least, the temporal characteristics of the laser /2/. By increasing the laser power density I_L an enhancement of the multiphoton ionization is obtained, while increasing the atom density N collisional processes in the vapor are amplified. It is not hard to image that by changing both I_L and N very complicated and interesting situations may be created; moreover this picture is further complicated by any molecules that are present in the vapor /3/.

Here we consider the experiments performed at low laser power density ($1-10 W cm^{-2}$) and low atom density ($10^{11}-10^{13} cm^{-3}$) while other processes are extensively treated elsewhere in this book. The first requirement assures that the multiphoton or processes induced by the laser field are negligible, the second that the secondary collisional processes, such as the electron superelastic collisions, are negligible. More precisely we consider the experiments where the dominant effects are the energy pooling collisions, i.e. the binary inelastic collisions of the type

$$A^*(np) + A^*(np) \rightarrow \begin{cases} A^{**}(nl) + A(ns) & a) \\ A_2^+ + e^- & b) \end{cases} \qquad (1)$$

where A(ns) is the alkali atom in the ground state, $A^*(np)$ is the laser excited state, $A^{**}(nl)$ is any excited state above the first and A_2^+ is the molecular ion. These collisions require, in the limit of a few kT, near resonance between the initial and final state energies.

These processes have been observed for the first time in sodium /4/ at $10^{12}-10^{13} cm^{-3}$ and very low laser intensity ($\lesssim 10 W cm^{-2}$); later on they have been recognized /5-7/ as the primary mechanism for producing both the seed electrons and the highly-excited states involved in the complete ionization experiments. The first example of this kind of experiment was succesful again in sodium /8/. Thus the energy pooling collisions deserve deep investigations not only for the understanding of the long range interactions in atoms, but also for the achievement of ionization with very moderate laser powers.

There are essentially three ways to detect the effects produced by a resonant laser excitation of a vapor: look at the fluorescence spectrum (i.e. detect the photons), detect the ions, either by collection of the total ion yield or by mass-resolved ion spectra, and collect the electrons. The detection apparatus can be considerably different in the three cases and also the geometry of the experiment has a fundamental influence on the results. The combination of these different techniques has given a substantial agreement on the phenomena investigated and we have now a qualitative picture of the general problem plus reliable quantitative results. In the first observation of process (1a) /4/ the apparatus was very simple and only the fluorescence spectrum was reported; in addition to the radiation from highly excited states observed in ref./4/, Leventhal and coworkers /9,10/ were the first to report, from the same experiment, also ion formation, both Na^+ and Na_2^+ produced by process (1b). The experimental conditions of ref./4/ and /9,10/ are basically the same, i.e. low atom density $\lesssim 10^{13} cm^{-3}$ and low laser power density $\lesssim 10 W cm^{-2}$; the two experiments proved that the excited states and the ions are produced by the same entrance channel, the collisions 3p+3p, which gives the energy transfer (1a) in the first case and the associative ionization (1b) in the second case. Ion analysis, with various tecniques for extraction and collection, have been used in sodium also by Carré et al. /11/. Merit of work /11/ is to have defined the values of laser power for which the laser field, although not strong enough to produce directly multiphoton ionization, may assist the simple associative ionization (1b) and the values of atom density for which the electron superelastic collisions become important. These results are also in good agreement with those obtained by Weiner and coworkers on beam experiments /12/. A definite proof of process (1) as the primary mechanism producing the low energy seed electrons has been given in ref./7/. This experiment is very important because it introduces, for the first time, electron spectrometry to resolve the energy spectrum of the electrons created in the vapor.

It is worth mentioning here that in the alkalis, $A^*(np) + A^*(np)$ connects to many electronic states A_2^{**} of the neutral molecule. The interesting side of this process is that the molecular states A_2^{**} have not necessarily the simmetry of a state allowed by dipole selection rules for one-photon absorption from the ground state of the dimer. Thus this collisional spectroscopy may be promising for producing triplet excited states of the alkali molecules /13/ and studying their possible application for new tunable laser sources.

II - RECENT EXPERIMENTS AND RESULTS

If the comprehension of the phenomena occurring in a dense vapor excited by resonant laser radiation is not straightforward because of their complexity, much more care has to be taken for a quantitative analysis. The first step is to perform the experiment with specific I_L and N to single out the process of interest; the energy pooling process (1) is usually made the dominant effect by reducing N and I_L. Then the main problem to proceed from the early qualitative observations to quantitative reliable measurements of the rate coefficients K or cross sections σ for processes (1a) and (1b), is the determination of the excited atom density N_{np}. An indetermination in excited atom density has indeed severe consequences on the values of K and σ because of the square dependence of the energy pooling processes from N_{np}, as can be easily shown by writing the rate equations. In the experiments where all the processes other than the energy pooling can be neglected the following simplified rate equation applies:

$$\dot{N}_{nl} = K_{nl} N_{np}^2 - N_{nl} \sum_{n'l'} A(nl,n'l') \qquad (2)$$

where N_{nl} is the population of the nl level, K_{nl} is the rate coefficient for process (1a) and A(nl,n'l') is the spontaneous transition probability for $|nl> \rightarrow |n'l'>$. Analogous equation can be written for process (1b) when the associative ionization rate coefficient K_{AI} has to be determined. Solution of eq.(2) at the steady-state gives

$$K_{nl} = <\sigma_{nl} v> = (N_{nl}/N_{np}^2) \sum_{n'l'} A(nl,n'l') \qquad (3)$$

where $v=\sqrt{8kT/\pi\mu}$ is the relative mean interatomic velocity. The quantity measured in the experiments is the intensity of the fluorescence lines or, more often, the intensity ratio of the emission from the highly excited state nl to the laser excited state np and from np to the ground state ns. The intensity per unit solid angle, I_{ik}, of a fluorescence line from level i to level k, as detected by the apparatus, is related to the population of level i through the relation

$$I_{ik} = \hbar \omega_{ik} A_{ik} N_i \epsilon_{ik} V/4\pi \qquad (4)$$

where ω_{ik} is the transition frequency, ϵ_{ik} is a factor which takes into account the instrumental response of the detecting apparatus and V is the fluorescence volume. In case of self trapping the natural radiative decay rate expressed by the spontaneous transition probability A_{ik} has to be changed with an effective rate which defines a trapped lifetime τ compared to the natural lifetime τ_0. Therefore the experiment involves also the determination of the effective laser-vapor interaction volume and the correct treatment of the radiation trapping phenomenon. Because of the self trapping, the apparent lifetime of the excited atom population increases, the diffusion of the excited atoms makes the interaction volume greater than the laser beam cylinder and also the radiation from the upper levels to the first p-level is attenuated with a change in the branching ratios of the higher nl-levels.

These difficulties have been overcome with various experimental approaches, that are briefly reviewed in the following while the results will be summarized in Table 1. Chéret et al. /14/, in their study of the Penning and associative ionization of 5p rubidium atoms with highly lying levels (6d,8s,7d), used the photoinization process

$$Rb(nl) + h\nu \rightarrow Rb^+ + e^- \qquad (5)$$

obtained with a second laser, to determine the concentration of the excited atoms. The same method was applied /15/ for the investigation of the energy pooling process

$$Rb(5p) + Rb(5p) \rightarrow Rb(5d) + Rb(5s) \qquad (6)$$

A cw dye laser ($\Delta\nu \approx 250$Hz and maximum power 250 mW) excites the rubidium atoms to the $5p_{3/2}$ level at a vapor density in the range $5\times10^{11} - 10^{13}$ cm^{-3}; thus the experimental conditions are similar to those of the previous experiments in sodium /4,9,10/. The population density of both the 5p and 5d levels is deduced from the measurement of the Rb^+ ion current produced through process (5) with a second cw Ar^+ laser that crosses the dye laser at right angles. By shifting the Ar^+ laser beam in a vertical plane also the spatial distribution of the excited states can be followed. The interaction volume is estimated by the overlapping of the two laser beams and absolute calibration of the ion current is made on a polarized plate inside the cell. The uncertainty on the rate coefficient for process (6) measured with this method (and reported in table 1) depends upon the accuracy of the photoionization cross-sections. Direct photoionization of the excited atoms has been used also in a beam experiment on sodium /16/ to measure the 3p atom density necessary for the determination of the associative ionization cross section for the process

$$Na(3p) + Na(3p) \rightarrow Na_2^+ + e^- \qquad (7)$$

The basic idea of this work is to get N_{3p} from the process

$$Na(3p) + h\nu \rightarrow Na^+ + e^- \qquad (8)$$

which gives a signal proportional to the 3p density, and to reduce the Na^+ production measurement to a ratio measurement of Na_2^+ and Na^+ densities. Measurement of an intensity ratio avoids the difficult determination of the absolute efficiency of the detecting apparatus, however, as we have already mentioned for the case of fluorescence detection, great care has to be taken to define the volume over which the signals are collected. In this particular experiment, for example, the volume for the Na^+ ions is simply defined by the laser beam that photoionizes the 3p atoms whereas the Na_2^+ ions, produced in process (7), are found in an enlarged effective volume created by the diffusion of the sodium atoms trapped in the 3p level. Another original way /17/ to measure excited state density in non-equilibrium, non steady-state situations is based on the increase of the trapped lifetime as a function of the total atom density. Leventhal and coworkers are now using this technique for Na(3p) determination in their experiments. Problems with early measurements (cfr. table 1) are probably related to the determination of the interaction volume in a cell that is not uniformely heated and not closed because of the holes for ion extraction.

This brief overview does not exhaust all the solutions devised in the different experiments, however we will consider only two more approaches, used for the specific measurement of the energy transfer cross section for the 5s and 4d levels of sodium, which are more relevant to the work reported in the next paragraph. The two methods are based on opposite basic idea: the first /18/ takes advantage of the self trapping to measure the spatial and temporal distribution of the excited atoms, the second /19/ makes an absolute calibration of the apparatus at low temperature when the self trapping is avoided. Huennekens and Gallagher /18/ have used pulsed excitation, tuned to the D_2 resonance line to produce the Na(3p) atoms ($I_L \cong 60\,\mu J$ in pulses of ~ 5nsec, $\Delta\lambda \cong 0.5 cm^{-1}$); the laser beam diameter is chosen in order to match the fundamental mode decay rate as a function of the time of the excited atom spatial distribution in presence of self trapping. A second laser, operating in cw single mode at very low power ($\sim 100\mu W$) and highly detuned from the D_2 line center ($\Delta\nu > 2.4$GHz) to avoid optical pumping distorsion, crosses at right angles the pulsed laser beam. The measurement of the change in transmission of the cw laser, following the pulsed excitation, is used to obtain the fraction of atoms in the 3p state as a function of time. The spatial distribution of 3p atoms is obtained by measuring the resonance fluorescence intensity and using the Holstein-vanTrigt theory /20/ for the diffusion across an infinite slab of trapped atoms. This theory applies correctly to this experiment because the geometry of the collision cell has been properly studied and the optical depths are high. Once the 3p atom density is known the rate constants for

$$Na(3p) + Na(3p) \longrightarrow Na(5s,4d) + Na(3s) \qquad (9)$$

are simply obtained by solving the rate equations of the process and by measuring the ratios of the transitions 5s-3p, 4d-3p and 3p-3s. The same technique for N_{3p} density determination has been employed /37/ also for the measurement of the associative ionization cross-section (process (7)). As noted before the volume integral of N_{3p}^2 and the N_{3p} density distribution is needed. Huennekens and Gallagher in this work have used two other independent methods for N_{3p} determination, one based on the total 3p-3s fluorescence intensity and the second on the ratio between 5s-3p and 3p-3s fluorescence intensity. The three techniques give results which agree within their uncertainties. In the experiment of ref./19/ the interaction volume is accurately determined in a capillary cell entirely illuminated by the laser beam (a broadband cw dye laser of low power $< 10 Wcm^{-2}$, tuned to the D_2 resonance line); the volume is also reduced to 4×10^{-4} cm^{-3} by a traseverse narrow slit ($\cong 150\mu m$). The Na(3p) atom density is determined first at low temperature T through the saturation of the resonance fluorescence and then at the temperature T', high enough to allow observation of process (9), simply by the relation

$$N_{3p}(T') = N_{3p}(T)\,\frac{I_{3p-3s}(T')}{I_{3p-3s}(T)}\,\frac{\tau^*}{\tau_0} \qquad (10)$$

The trapped lifetime τ^* of the 3p level is correctly given in this experiment by the Milne theory /21/ which, contrary to the Holstein-vanTrigt treatment, is valid for thin optical depths. Having the N_{3p} value, the rate constants for process (9) are determined, as in the approach of Huennekens and Gallagher, by measuring fluorescence intensity ratios. The results of these two experiments have settle

of energy pooling cross sections for other alkalis.

Special attention deserves the experiment of Le Gouët et al. /7/. Although the relevant aim of this work is the direct observation of the superelastic collisions, that are outside our subject, it also shows unambiguously the role of the energy pooling processes in the production of the seed electrons. Sodium atoms in a beam of density 10^{13} cm^{-3} are excited to the $3p_{3/2}$ level by a cw dye laser of low intensity ($\approx 3 Wcm^{-2}$). The multiphoton or laser assisted processes are then completely negligible as in the experiment of ref. /4,9,10/. The detection apparatus consists of a cylindrical mirror analyzer that resolves the energy spectrum of the electrons emerging from the interaction zone. These spectra contain a number of peaks corresponding to the low-energy electrons produced by the associative ionization and to electrons created from the various excited states by the ionizing collisions

$$Na(3p) + Na(nl) \longrightarrow Na(3s) + Na^+ + e^- \qquad (11)$$

In particular peaks at energy values of electrons coming from atoms in the 5s and 4d states have been identified and an indirect estimation of the energy transfer cross-sections σ_{5s} and σ_{4d} has been made. The low energy electrons are then heated by one or more superelastic collisions leading to further ionization. However the interesting point from our point of view is that, in the conditions of low power laser intensity and relatively low atom density, the dominant processes are purely collisional.

The energy pooling processes have not received so far much attention from a theoretical point of view; for sodium, to which so many experiments have been devoted, there is only the calculation by Kowalczyk /22/ who considered the single process

$$Na(3p) + Na(3p) \longrightarrow Na(4d) + Na(3s) \qquad (12)$$

He uses a model first introduced by Borodin and Komarov /23/ for the calculation of the cross section for collision between two 6p caesium excited atoms. This model considers the adiabatic terms for the quasi molecule Na_2 corresponding to the configurations 3p+3p and 3s+4d and it is valid only for large interatomic distances ($R > 20$a.u.) because of the asymptotic approximations made. In the interaction Hamiltonian only the terms important at large distance, namely the exchange and dipole-dipole interactions, are taken into account. The contribution of ion-pair configurations is also neglected and the eigenfunctions are not orthogonalized. The error so introduced is minor for $R > 35$ a.u. but it is important at shorter distances. Nevertheless the order of magnitude of the cross section calculated by Kowalczyk matches the experimental results, as shown in table 1. The same method has been applied by Barbier and Chéret /15/ for the calculation of the cross section relative to process (6). This is a more favourable case than the one studied by Kowalczyk because the energy defect ($\Delta E \cong 68 cm^{-1}$) is small and the main contributions come in the validity range of the model. Barbier and Chéret consider also the ionic ($Rb^+ + Rb^-$) crossing curves for both the configurations 5p+5p and 5d+5s; however this contribution is negligible in the Rb(5p)+Rb(5p) reaction. The agreement between experimental and theoretical values is certainly better (cfr. table 1) for rubidium than sodium. However ab initio calculations of the potential energy curves for diabatic molecular states connecting to 3s+nl (with nl=3s,4s,5s,3p,4p,3d,4d and 4f) and

3p+3p are in progress for sodium /24/. These calculations are considered "complete" because both the Multi-Configuration-Self-Consistent-Field energy and the remaining energy of electronic correlation are calculated. The MC-SCF energy is obtained by an integrated density functional; then the coupling matrix elements for the various states are constructed and reliable quantitative determinations for all the energy pooling collisions from 3p+3p to the levels mentioned above are to be expected.

III - AN UPDATE EXPERIMENT IN SODIUM

In sodium, beside the 5s and 4d, there is the level 4f which is close in energy to 3p+3p; as an immediate extension of our early work, we have now measured the cross section for the process

$$Na(3p) + Na(3p) \longrightarrow Na(4f) + Na(3s) \qquad (13)$$

This measurement was not done before mainly because the emission of the 4f state is in the near infrared (1.84 μm), a region far beyond the sensitivity of the optical apparatus used in previous experiments. However process (13) is of particular interest because the 4f state lies very close to the 4d ($\Delta E \simeq 38 cm^{-1}$), therefore we get also informations on the process

$$Na(3s) + Na(4d) \underset{K'}{\overset{K}{\rightleftharpoons}} Na(3s) + Na(4f) \qquad (14)$$

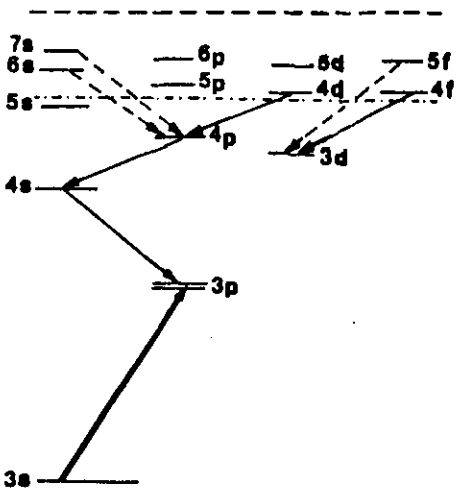

	λ(μm)
4s-3p	1.14
5f-3d	1.26
7s-4p	1.29
6s-4p	1.63
4f-3d	1.84
4p-4s	2.20
4d-4p	2.33

Fig. 1 - Simplified energy level scheme of Na. The dashed line corresponds to the ionization limit and the dashed-dotted line to twice the energy of the 3p level. The arrows correspond to the transitions observed in this experiment; the transitions indicated with a dashed line are present only in the cell with buffer gas.

Our apparatus has been sligthly modified to include a monochromator with a grating for the infrared and a PbS detector for the near infrared. The laser used to excite the sodium atoms to the $3p_{3/2}$ level is a single mode dye laser of maximum power 120mW and actively stabilized to a $\Delta\nu \cong 1MHz$, with a frequency drift of less than ≅100MHz/hour. A single mode dye laser is not necessary in principle, however its stability characteristics have reduced the fluctuations of the laser intensity. To improve the signal-to-noise ratio the laser beam has been modulated and phase sensitive detection has been used. Further a second chopper has been used to switch on/off the beam at very low frequency (~0.4Hz); the same function generator which drives the chopper also triggers a multichannel analyzer system used for signal averaging. With $N=2^6$ cycles recorded on the multichannel analyzer the statistical error decreases of a factor $1/\sqrt{N} = 1/2^3$. At the end of each cycle the signal was displayed on the analyzer and chart recorded. Since each recording on the multichannel analyzer lasted 5sec the single mode dye laser has been very useful to keep the excitation stable on the maximum of the D_2 line. As usual in our experiments the quantity measured is the intensity of the fluorescence lines. In figure 1 a scheme of the energy levels involved are reported with the observed transitions. We have used two cells, one with pure sodium and a second containing sodium plus a few torr of a buffer gas. The temperature has been kept to the lowest values allowing detection of the fluorescence from the desired levels without having fluorescence from higher levels which assures that the secondary collisional or ionizing processes are avoided. The cross section σ_{4f} for process (13) has been determined relatively to σ_{4d}, that was measured in an "absolute" way, as mentioned before /19/. This approach is reasonable because the volume from which we observe the fluorescence of the 4d and 4f levels is the same, the laser intensity is stable and no radiation trapping is present for these high levels. Moreover the emission 4d-4p is in the same near infrared spectral range of the 4f-3d emission so that we can measure their intensities with the same detecting apparatus and obtain directly the population ratio of the 4d and 4f levels. The relation between N_{4f} and N_{4d}, necessary for the determination of K_{4f} and K_{4d}, has been obtained by solving the rate equations in steady-state conditions for both levels. The complete treatment includes processes such as radiative decay from higher levels, electron impact ionization, photoionization and Penning ionisation in collisions with 3p atoms and the solution is rather complicated. However in our experiment we have worked with atom density and laser power density low enough to make these terms negligible; we have instead taken into account the exchange term 4f-4d. The equations are therefore

$$\dot{N}_{4d} = (A(4d,3p)+A(4d,4p))N_{4d} + K_{4d}N_{3p}^2 - KNN_{4d} + K'NN_{4f} \qquad (15)$$

$$\dot{N}_{4f} = A(4f,3d)N_{4f} + K_{4f}N_{3p}^2 + KNN_{4d} - K'NN_{4f} \qquad (16)$$

where K and K' are the rate coefficients of process (14); they are related to each other /25/ through the level degeneracy $K/K' = (g_{4f}/g_{4d})\exp(-\Delta E/kT) = 1.26$. The solution of eq.(15) and (16) at the steady-state yields for the population ratio

$$\frac{N_{4f}}{N_{4d}} = \frac{(A(4d,3p)+A(4d,4p)+KN)^2K_{4f} + (A(4d,3p)+A(4d,4p)+KN)KK_{4d}N}{((A(4d,3p)+A(4d,4p)+KN)(A(4f,3d)+K'N)-KK'N^2)K_{4d}+(A(4d,3p)+A(4d,4p)+KN)K_{4f}+KK_{4d}N)K'N} \qquad (17)$$

The value N_{4f}/N_{4d}, for a fixed laser intensity and a given temperature, i.e. for a specific atom density N, is obtained by measuring the intensity ratio I(4f,3d)/I(4d,4p) and using relation (4); K_{4d} can be taken from ref./18/ or /19/. Then we can fit eq.(17) to the parameters K_{4f} and K. For $K_{4d}=(3.0\pm0.9)\times10^{-10}$ cm^3 sec^{-1} the best fit has given the values

$$K_{4f} = (5.6\pm2.2)\times10^{-11}\ \text{cm}^3\,\text{sec}^{-1} \quad ; \quad K = (9.8\pm4.9)\times10^{-9}\ \text{cm}^3\,\text{sec}^{-1}.$$

In figure 2 the data for N_{4f}/N_{4d}, with the best fit curve, are reported as a function of the temperature.

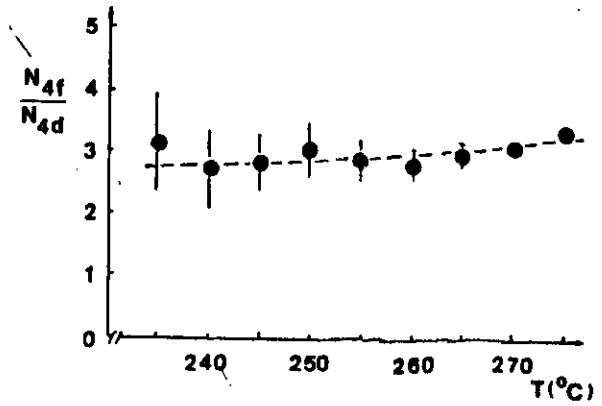

Fig. 2 - N_{4f}/N_{4d} ratio versus temperature. The dots represent the data and the dashed curve the best fit to eq. (17).

The indetermination on K shows, as expected, that this experiment is not the best way to investigate process (14); a simple way to perform this experiment would be to excite by two photon the transition 3s-4d and then detect the sensitized fluorescence 4f-3d. In this context, however, it is more interesting to see the variation of K_{4f} when the exchange collisions 4f-4d are neglected. In this case the solution of the simplified rate equations yields

$$K_{4f}/K_{4d} = (N_{4f}/N_{4d})((A(4f,3d)/A(4d,3p)+A(4d,4p))) \qquad (18)$$

which gives the value $K_{4f} = (6.0\pm2.4)\times10^{-11}$ cm^3 sec^{-1}. It is evident that the effect of process (14) on K_{4f} is not very strong at the temperatures of our experiments; since K_{4d} is about one order of magnitude bigger than K_{4f} this effect is even less important and this fully justifies why in both the experiments of ref./18/ and /19/ was neglected. At higher temperatures, however, the exchange 4d-4f increases and according to what observed by Huennekens and Gallagher and to our results shown in figure 2 seems to depopulate the 4d level. The theoretical work which is in progress /24/ is expected to be accurate enough to explain also

($\sigma_{4d}=(3.2\pm1.1)\times10^{-15}$ cm^2 compared to $\sigma_{4f}=(5.7\pm2.3)\times10^{-16}$ cm^2 at T=250°C); as a first comment we may say that the selection rules apparently favour the collisions where the total atomic angular momentum is unchanged. Our combined results for σ_{5s}, σ_{4d} and σ_{4f} indicates that the production of 3d atoms (fluorescence from the 3d, level was observed in ref./4/ as one of the most intense) is through cascade from 4d and 5s via the 5p level and direct radiative decay from the 4f level, which is in contrast with the results of Krasinski et al. /26/.

Similar investigations with a cell containing a buffer gas have given signals from higher levels, such as the 5f. Power dependence (see for example figure 3 regarding the 5f level) indicates that these levels are primarily populated not by energy transfer collisions

$$Na(3p) + Na(3p) \longrightarrow Na(5f) + Na(3s) \qquad (19)$$

but rather through recombination. Neverthless, since fluorescence from the 5f level was not observed in the cell without buffer gas, we can give an upper limit to the rate coefficient of process (19): $K < 10^{-13}$ cm^3 sec^{-1}.

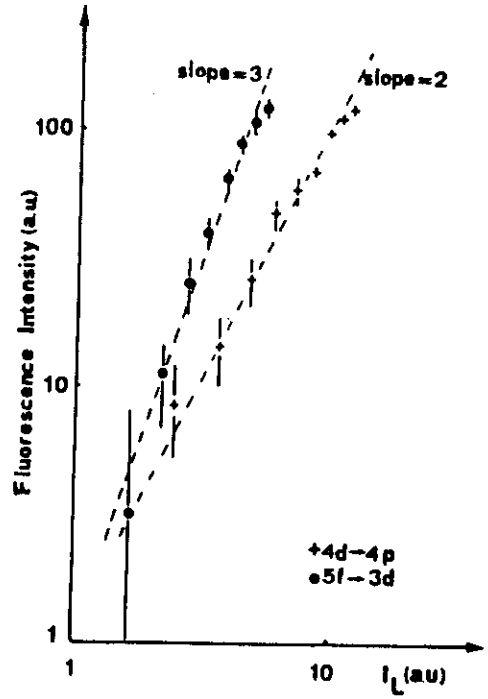

Fig. 3 - Log-log plot of the fluorescence intensity for the transitions 4d-4p and 5f-3d versus laser power. The intensities are normalized independently and the maximum laser power is 60mW. It is evident the square dependence of the 4d-4p transition and the cubic dependence of the 5f-3d transition.

IV - CONCLUSIONS

Since the first observations of energy pooling processes in laser-irradiated alkali vapors a great deal of work by many research groups has yield a clear insight of the phenomenon and reliable quantitative results. For convenience we report in the following table the values for energy transfer and associative ionization cross sections in the alkalis, updated to include the most recent results we are aware of:

TABLE 1. ENERGY POOLING CROSS SECTIONS OF ALKALI METAL ATOMS

A. Energy Transfer

Alkali Metal	Reaction	Energy Defect (cm^{-1})	T (°K)	σ_2 (cm^2)	Reference Exp.	Reference Theor.
Na	Na(3p)+Na(3p)→					
	→ Na(5s)+Na(3s)	+746	~487	7.3×10^{-20}	27	
			597	$(1.6 \pm 0.6)\times10^{-15}$	18	
			483	$(2.0 \pm 0.7)\times10^{-15}$	19	
	→ Na(4d)+Na(3s)	-602	670	9×10^{-18}	28	
			~487	4.7×10^{-20}	27	
			beam	$\sim10^{-14}$	7	
			~597	$(2.3 \pm 0.8)\times10^{-15}$	18	
			483	$(3.2 \pm 1.1)\times10^{-15}$	19	
			550	2.3×10^{-16}		22
			550	1.2×10^{-15}		29
	→ Na(6s)+Na(3s)	-2426	~597	6×10^{-17}	18	
				2.3×10^{-17}	(c)	
	→ Na(5d)+Na(3s)	-3090	~597	1×10^{-16}	18	
				3.8×10^{-17}	(c)	
	→ Na(4f)+Na(3s)	-642	523	$(5.7 \pm 2.3)\times10^{-16}$	present work	
	→ Na(5f)+Na(3s)	-3110	533	10^{-18}	present work	
K	K(4p)+K(4p)→					
	→ K(6s)+K(4s)	-1365	483	6×10^{-16}	6(a)	
	→ K(4d)+K(4s)	-1312	483	8×10^{-16}	6(a)	
Rb	Rb(5p)+Rb(5p)→					
	→Rb(5d)+Rb(5s)	-68	450	$(3 \pm 1.5)\times10^{-14}$	15	
				1×10^{-14}		15
Cs	Cs(6p)+Cs(6p)→					
	→Cs(6d)+Cs(6s)	-300	528	10^{-13}	30	
			220	2.8×10^{-14}		15(b)
			1000	$0.2 - 2 \times 10^{-14}$		23

B. Associative Ionization

Li	Li(2p)+Li(2p)→ $\rightarrow Li_2^+ + e^-$	~3300	900	5×10^{-20}	32
Na	Na(3p)+Na(3p)→ $\rightarrow Na_2^+ + e^-$	≈400	575	$(3.7 \pm 0.4)\times10^{-16}$	33
			≈500	1×10^{-15}	9
			beam	5×10^{-18}	34
			≈500	2×10^{-17}	10
			≈500	1.4×10^{-17}	35
			beam	$(1.5 \pm 0.6)\times10^{-16}$	36
			≈650	$(8.1 \pm 1.9)\times10^{-17}$	37
K	K(4p)+K(4p)→ $\rightarrow K_2^+ + e^-$	≈1700	450	$(1.3 \pm 0.3)\times10^{-17}$	38
Rb	Rb(5p)+Rb(5p)→ $\rightarrow Rb_2^+ + e^-$	≈1600	473	$(6.6 \pm 0.8)\times10^{-18}$	39
Cs	Cs(6p)+Cs(6p)→ $\rightarrow Cs_2^+ + e^-$	≈3000	500	$(7 \pm 5) \times10^{-18}$	40
			450	$(1.1 \pm 0.3)\times10^{-15}$	41
			425	$(5.4 \pm 0.5)\times10^{-18}$	42

a) Deduced from the fluorescence intensity ratios I(6s-4p)/I(4p-4s) and I(4d-4p)/I(4p-4s) measured in ref./4/.
b) Deduced from the result of ref./31/ for the process $Cs(6d_{3/2}) + Cs5s_{1/2}) \rightarrow Cs(6p) + Cs(6p)$.
c) Obtained from the absolute value of σ_{5s} of ref./18/ and the relative intensities given in ref./4/ at T=593°K.

REFERENCES

1. See for example: "Photon-Assisted Collisions and Related Topics" Eds. N.K.Rahman and C.Guidotti, Harwood Academic Publishers,1982; "Collisions and Half-Collisions with Lasers" Eds. N.K.Rahman and C.Guidotti, Harwood Academic Publishers, 1984
2. Allegrini M., Garver W.P., Kushawaha V.S. and Leventhal J.J., Phys.Rev. A28 (1983) 199

3. Lucatorto T.B. and McIlrath T.J., Appl.Opt. 19 (1980) 3948; Kopystyńska A. and Moi L., Phys.Rep. 92 (1982) 135
4. Allegrini M., Alzetta G., Kopystynska A., Moi L. and Orriols G., Opt.Comm. 19 (1976) 96
5. Allegrini M., Gozzini S., Longo I., Savino P. and Bicchi P., Nuovo Cimento D1 (1982) 49
6. Giammanco F. and Gozzini S., Nuovo Cimento B66 (1981) 47
7. Le Gouët J.L., Picqué J.L., Wuilleumier F., Bizeau J.M., Dhez P., Koch P. and Ederer D.L., Phys.Rev.Lett. 48 (1982) 600
8. Lucatorto T.B. and McIlrath T.J., Phys.Rev.Lett. 37 (1976) 428
9. Bearman G.H. and Leventhal J.J., Phys.Rev.Lett. 41 (1978) 1227
10. Kushawaha V.S. and Leventhal J.J., Phys.Rev. A22 (1980) 2468
11. Carré B., Roussel F., Breger P. and Spiess G., J.Phys.B: At.Mol.Phys. 14 (1981) 4271; 14 (1981) 4289
12. Weiner J. and Polak-Dingels P., J.Chem.Phys. 74 (1981) 508
13. Allegrini M. and Moi L., Opt.Comm. 32 (1980) 91
14. Chéret M., Barbier L., Lindinger W. and Deloche R., J.Phys.B: At.Mol.Phys. 15 (1982) 3463
15. Barbier L. and Chéret M., J.Phys.B: At.Mol.Phys. 16 (1983) 3213
16. Bonanno R., Boulmer J and Weiner J., Phys.Rev. A28 (1983) 604
17. Garver W.P., Pierce M.R. and Leventhal J.J., J.Chem.Phys. 77 (1982) 1201
18. Huennekens J. and Gallagher A., Phys.Rev. A27 (1983) 771
19. Allegrini M., Bicchi P. and Moi L., Phys.Rev. A28 (1983) 1338
20. Holstein T., Phys.Rev. 72 (1947) 1212; 83 (1951) 1159; Van Trigt C. Phys.Rev. 181 (1969) 97
21. Milne E.A., J.London Math.Soc. 1 (1926) 40
22. Kowalczyk P., Chem.Phys.Lett. 68 (1979) 203; 74 (1980) 80
23. Borodin V. and Komarov I.V., Opt.Spectrosc. 36 (1974) 145
24. Colle R. and Salvetti O., private communication
25. Hasted J.B., Physics of Atomic Collisions, London Butterworths,1972
26. Krasinski J., Stacewicz T. and Stroud C.R., Opt.Comm. 33 (1980) 158
27. Kushawaha V.S. and Leventhal J.J., Phys.Rev. A25 (1982) 570
28. Krebs D.J. and Schearer L.D., J.Chem.Phys. 75 (1981) 3340
29. Kowalczyk P., J.Phys.B: At.Mol.Phys. 17 (1984)
30. Klucarev A.N. and Lucatorto A.V., Opt.Spectrosc. 32 (1972) 576
31. Yabuzaki T., Tam A.C., Hou M., Happer W. and Curry S.M., Opt.Comm. 24 (1978) 305
32. Hellfeld A.V., Caddick J. and Weiner J., Phys.Rev.Lett. 40 (1978) 1369
33. Klucharev A., Sepman V. and Vuinovich V., Opt.Spectrosc. 42 (1977) 336
34. De Jong A. and Van der Valk F., J.Phys.B: At.Mol.Phys. 12 (1979) L561
35. Kushawaha V.S. and Leventhal J.J., Phys.Rev. A25 (1982) 346
36. Bonanno R., Boulmer J. and Weiner J., Phys.Rev. A28 (1983) 604
37. Huennekens J. and Gallagher A., Phys.Rev. A28 (1983) 1276
38. Klukarev A., Sepman V. and Vuinovich V., J.Phys.B: At.Mol.Phys. 10 (1977) 715
39. Borodin V.M., Klyucharev A.N. and Sepman V.Yu, Opt.Spectrosc. 39 (1975) 231
40. Alfredo G. and Kniazzch A., Bull.Am.Phys.Soc. 11 (1966) 634
41. Klyucharev A.N. and Ryazanov N.S., Opt.Spectrosc. 33 (1972) 230
42. Dobrolezh B.V., Klyucharev A.N. and Sepman V.Yu, Opt.Spectrosc. 38 (1975) 630

H. Hefdt and K. Jaworowski Eds., (World Scientific Publ., 1988)

EXPERIMENTS ON LASER EXCITED ALKALI VAPORS*

MARIA ALLEGRINI

Istituto di Fisica Atomica e Molecolare del C.N.R.
Via del Giardino 7, 56100 Pisa, Italy

ABSTRACT

In these lectures a short review of some experiments dealing with the interaction of laser light with alkali metal vapors is presented. Due to a favourable combination of properties, alkali atoms and molecules are ideal systems for guide experiments in physics, sometimes testing simple and fundamental ideas. The experiments reported here involve the combined effects of laser excitation and collisional processes.

1. INTRODUCTION

The atoms and the diatomic molecules of the alkali metals have several properties for which they have been used in many experiments to test fundamental ideas in physics, eventually extended to other systems for interesting applications. These properties are well known and have been extensively reviewed, for example by Stwalley and coworkers [1]. To mention just a few of these characteristics, alkali atoms and molecules have a simple hydrogen-like structure convenient for easy theoretical analysis, their ionization potential is so low, compared for example to hydrogen, that efficient plasma generation is easily achieved by photoionization or collision-aided ionization and their interaction with electromagnetic radiation is very strong, particularly in the region where commercial tunable dye lasers have been available for long time.

In our laboratory we also have taken advantage of the favourable properties of the alkali metals to conduct several experiments involving alkalis in the gas phase excited

---

*Presented at the XV International Summer School on Quantum Optics, Poland, September 1987.

by laser light. Some of these experiments will be reported in the following, with special attention to cases where collisional processes play an important role. A common scheme for all our experiments is shown in figure 1.

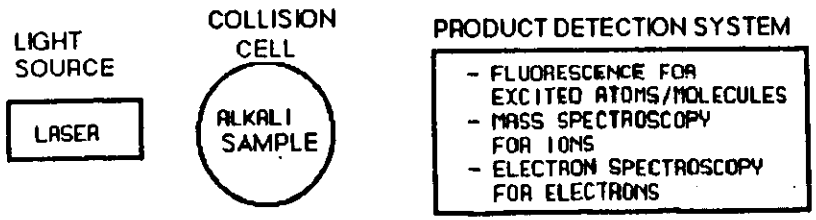

Figure 1. Schematic for typical collision experiments in laser excited alkali vapors.

The interaction light is produced by commercial or laboratory made lasers in the visible, cw or pulsed, broadband or single mode, depending on the requirements of the specific experiment. The sample is an alkali saturated vapor, i.e. in equilibrium with its corresponding liquid condensed phase. The alkali metals are solid at room temperature and an easy way to produce the saturated vapor is to heat, well below the boiling point, a piece of solid distilled and sealed in a cell in high vacuum conditions. Under the assumption of thermal equilibrium the atom density of the saturated vapor can be conveniently determined from the temperature of the cell, using the Nesmeyanov tables [2] for the vapor pressures. Unfortunately the alkali metals are very reactive chemical elements which, with increasing temperature, attack most optical materials and therefore the vapor pressure depends also from the interactions and the distribution of the alkali metal on the cell surface. Ordinary pyrex cells are useful only for experiments at low atom density when chemical reactions with the glass are not too severe. When we have determined the atom density from the temperature we used to bake the glass cells at low temperature for several days before use to help the achievement of thermal equilibrium inside the cell. There are other techniques to prepare and to confine alkali vapors such as atomic or molecular beams [3] and heat pipe ovens [4]. There are also several methods, usually based on the vapor-resonant light interaction, to determine the atom density with high precision and some of these methods [5,6,7] are expressly appropriate to experiments like ours. When we have worked with pure alkalis the atom density has been determined directly from the temperature of the cell within a 10-15% accuracy; however for the experiments treating alkali mixtures [8,9,10] the atom density determination has been a serious problem and we have been forced to use one of the more precise techniques [5]. The detection apparata used in our experiments vary depending upon the products to be detected. It may be as simple as a monochromator plus a photomultiplier to disperse and to detect fluorescence emissions or it may be sophisticated as a quadrupole mass spectrometer plus particle multiplier to identify ions.

Let us now illustrate some specific experiments in which we have observed the formation of diatomic alkali molecules in presence of optical pumping of the atoms, the collisions between two alkali atoms, laser excited to the first P-resonance level, the collisions involving laser produced atoms in high-lying states (Rydberg atoms), and the mechanical action exerted by the laser light on the motion of alkali atoms in a capillary cell.

2. ALTERATION OF THE ATOM-DIMER EQUILIBRIUM

An alkali vapor in thermal equilibrium with its liquid metal is made essentially of single atoms A and a few percent of diatomic molecules A_2, while concentration of polyatomic molecules A_n is much lower with increasing number n of atoms. In stationary regime the reaction atoms/dimers is simply described by

$$A + A \underset{}{\overset{k}{\rightleftharpoons}} A_2 \qquad (1)$$

and can be seen as a collisional process with rate constant k. In principle the equilibrium between atoms and molecules depends only upon their densities, i.e. k is only temperature dependent as

$$k(T) = N_m / N_a^2 \qquad (2)$$

where N_m and N_a are the molecule and atom density.

Like hydrogen molecules H_2, the alkali diatomic molecules have two electrons outside two inert ionic cores, which originate two electronic molecular states: the $^1\Sigma_g^+$ state when the electron spins point in opposite directions and the $^3\Sigma_u^+$ state when the spins are aligned. These two electronic states at large internuclear distances R separate in two ground state atoms, as indicated in figure 2.

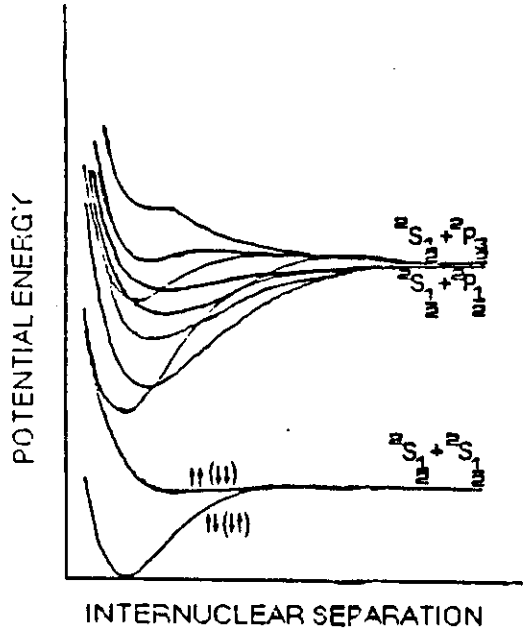

Figure 2. Qualitative potential curves for homonuclear alkali dimers in the ground and first excited manyfold. The corresponding atomic dissociation products are indicated. For the ground states the arrows indicate the mutual orientation of the electron spin.

The singlet state is bound by typically 5000 cm^{-1}, while the triplet state is mostly repulsive. Thus it is evident that when two ground state atoms with antiparallel spins approach each other they interact along an attractive potential curve and form the molecule, while molecule formation is inhibited when two approaching atoms with parallel oriented spins collide along an antibonding repulsive potential. In other words the dimerization equilibrium constant k (T) must also depend upon the degree of atomic orientation inside the vapor, S. S is defined as

$$S = (N_u - N_d) / (N_u + N_d) \qquad (3)$$

where N_u is the density of atoms with spin "up", N_d is the density of atoms with spin "down" and obviously $N_u + N_d = N_a$ is the total atom density.

Bernheim [11] first suggested that the reaction $2Rb \dashrightarrow Rb_2$ could be shifted to the left by preparing all Rb atoms with parallel oriented spins by the already well established optical pumping technique [12]. Kastler performed the detailed mathematical analysis [13] of the influence of atomic orientation on molecule formation and gave the following relationship for the rate constant

$$k(S,T) = k(0,T)(1 - S^2) \qquad (4)$$

where k (0, T) is the rate constant in absence of atomic orientation. Thus

$$N_m = k(0,T) N_a^2 (1 - S^2) = N_{0m} (1 - S^2) \qquad (5)$$

where $N_{0m} = k(0,T) N_a^2$ is the maximum value of the molecular density at the temperature T reached when the degree of atomic orientation is zero, that is, when the spins are not oriented.

The inhibition of molecule formation has been detected through the decrease of the fluorescence intensity induced by a laser resonant with a molecular transition from the ground singlet state. To our knowledge no successful experiments have yet been reported on the shifting of the dimerization reaction to the right, or, in other words, on the increase of the number of diatomic molecules by preparing the atoms with their spins oriented in opposite directions. This fact is not surprising because of the practical difficulties encountered in these kind of experiments that in principle are so simple. The main problem is that at the temperatures where there is a sufficiently large number of molecules to allow a reasonably easy detection of molecular fluorescence, the degree of atomic orientation to produce an appreciable effect on the dimer density is very poor. In a theoretical simplified picture there are also other difficulties: the systems we are treating are not pure spin 1/2 systems, the polarization of the atoms influences also the relative abundances of ortho- and para- molecules because of the atom-dimer nuclear polarization transfer, population density of molecular levels could be modified by molecular alignment produced by the alignment of the atoms forming the molecules and so on. However sophisticated theoretical treatments could certainly take into account these problems; here only the experimental results are reported.

Fluorescence decrease of potassium molecules K_2 was detected by Alzetta et al. [14] in presence of potassium atoms oriented by spin exchange with optically pumped

sodium atoms. The mixture of sodium plus potassium gave at a certain temperature the best density for Na optical pumping and a reasonable density of K_2 molecules to observe their fluorescence. Use of a laser instead of a lamp as light source has made possible experiments on pure alkali vapors [15,16] with control of the dependence of the atom/dimer equilibrium constant k upon the atomic degree of orientation S [17]. A summary of all experiments and results obtained in Pisa can be found in reference [18]. For the schematic of the experiment we refer to figure 1 of reference [17]. The experiment uses a mixture of sodium and potassium plus 130Torr of neon contained in a cell sealed under vacuum. A foreign buffer gas helps the optical pumping process and also serves as a third body balance in the dimerization reaction. The optical pumping of the sodium atoms is done with a cw dye laser circularly polarized and tuned to the D_1 resonance line in a weak and uniform magnetic field parallel to the laser beam. The degree of atomic orientation is measured through Faraday rotation, as proposed by Gozzini [19]. An oriented vapor becomes an optical active medium with different indices of refraction n'_- and n'_+ for right σ_- and left σ_+ circularly polarized light. The plane of polarization of a linear polarized probe laser beam crossing the oriented vapor rotates of a quantity $\Delta\theta$, the Faraday rotation angle. It is well known that $\Delta\theta$ is given by

$$\Delta\theta = [\pi(n'_- - n'_+) l] / \lambda \qquad (6)$$

where l is the thickness of the vapor crossed by the laser and λ the laser wavelength. In our case the weak probe laser wavelength was inside the absorption profile of the D_1 resonance line, sligthly detuned from the line center. An example of these rotation signals is shown in figure 3.

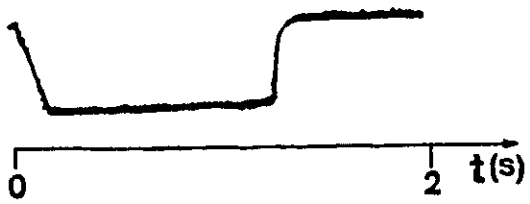

Figure 3. Typical rotation signal for sodium D_1 line during a full pumping cycle.

The sodium molecules are excited by an Ar^+ laser and changes of molecular density are inferred from laser induced fluorescence. A typical signal showing the decrease of Na_2 fluorescence during an optical pumping cycle and the corresponding increase during a relaxation cycle when the atomic orientation is destroyed is shown in figure 4.

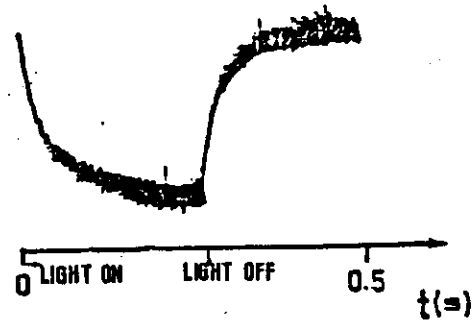

Figure 4. Na_2 fluorescence variation during a pumping and a relaxation cycle of the atoms (from ref. [17]).

The same effect was observed in potassium while the atoms were pumped by spin-exchange collisions with the laser oriented sodium atoms.

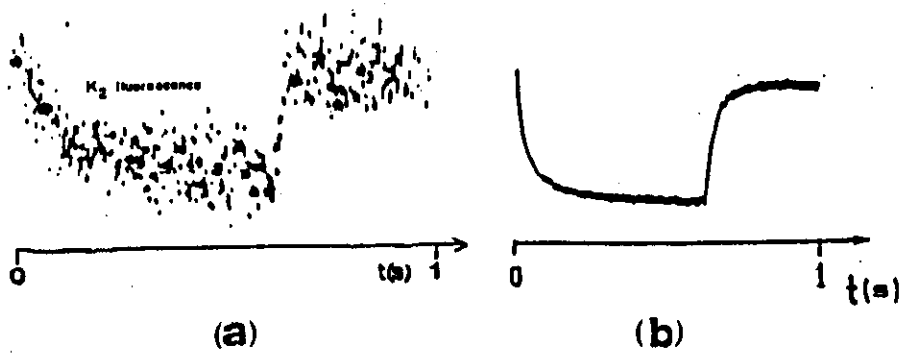

Figure 5. K_2 fluorescence variation when optical pumping source is a lamp (a), from ref. [14] and a laser (b), from ref. [17].

In figure 5 K_2 fluorescence signals obtained with a lamp as pumping source (fig.5a) and a laser (fig. 5b) are reported for comparison. For sodium, using the signals of figures 3 and 4, normalized to the total variation, it is easy to construct plots of the function $(1 - S^2)$ versus time, for both the pumping and the relaxation cycles of the optical pumping phenomenon. As it is evident from figure 7 of reference [17] the molecular fluorescence variation fits the $(1 - S^2)$ curve very well. For a direct check of the validity of relation (5) it is convenient to look at the molecular density change $N_m (S)/N_{0m}$ versus S, as shown in figure 6 of reference [18]. A direct measurement of Na/K spin-exchange rate was outside the aims of the experiment, otherwhile the same check could be possible also for potassium.

These experiments have conclusively demonstrated that the atom/dimer equilibrium is affected by the optical orientation of the colliding reactants and thus they open the possibility of optical control of a chemical reaction. In this sense they may be seen as complementary to the experiments on spin-polarized hydrogen by magnetic confinement at very low temperature [20,21].

3. COLLISIONS IN LASER IRRADIATED VAPORS

Irradiation of dense alkali vapors with laser light resonant with the fundamental $S_{1/2}$ ---> $P_{1/2}$ or $S_{1/2}$ ---> $P_{3/2}$ transition produces a high concentration of excited states that allowes the observation of the collisions between two atoms, both in the excited state. The first two experiments were reported in 1976 showing total ionization consequent to formation of seed electrons by associative ionization [22] and fluorescence from higher levels populated through the collisions [23]. While the physics of atomic collisions was previously devoted to the study of reactions involving one ground state atom and only one excited atom, usually in a metastable state, these two experiments, that joint the spectroscopy and scattering techniques, have started a rapidly growing field of research. More recently much interest has arised also for collisions involving atoms in a state with a large quantum number n (Rydberg atoms). Here we will see some features, first of the collisions between two alkali atoms in the first excited state and later of heavy body collisions involving very excited atoms.

3.1. Collisions between alkali atoms excited to the first P-resonance level

Collisions between alkali atoms A^*, laser excited to the first P-level, have several reaction channels with rate constants k or cross sections σ that can be outlined as

$$A^* + A^* \xrightarrow{k_{ET},\ \sigma_{ET}} A^{**} + A \qquad (7a)$$

$$\xrightarrow{k_{AI},\ \sigma_{AI}} A_2^+ + e \qquad (7b)$$

$$\xrightarrow{k_{MF},\ \sigma_{MF}} A_2^{**} \qquad (7c)$$

where A is a ground state atom, A^{**} is a highly excited atom whose energy is close to twice the A^* energy, A_2^+ is the molecular ion and A_2^{**} is the diatomic molecule in an excited electronic state. The collision $A^* + A^*$ can be seen as an atom-atom electronic energy transfer during the interaction when the two atoms approach each other. This interaction for slow collisions is well described by the molecular adiabatic potentials. Clearly there are many of these potential curves corresponding to $A^* + A^*$ entrance channel and the exit channels are defined by the series of crossings, or more properly of "avoided crossings", in the potential energy curves corresponding to the final products. Since the collisions are thermal the energy balance between entrance and and exit channel is provided by the kinetic energy of the reactants and products and then ΔE is of the order of few kT.

Important parameters for these processes are the atom density N and the laser power density I. In the experiments described here the vapors are dense, however N is kept in the range 10^{11}-10^{13}cm^{-3} in order to avoid superelastic collisions or secondary collision processes. The laser power density is low, from few mW/cm^2 to 10^3W/cm^2, so that multiphoton or laser induced processes are negligible. The laser is tuned to the S-->P resonance transitions and it merely serves as a tool to prepare the excited reactants for the collisions. When the laser is cw a steady-state concentration of potential reactants is produced, while under pulsed irradiation the laser pulse duration becomes important and different results are obtained for example passing from a 10nsec to a 1μsec laser pulse [24]. It is important to underline that the collisions we are treating are thermal, with a collision duration of the order of 10^{-12}-10^{-13}sec given roughly by the ratio atom dimension/thermal velocity. The rate coefficients for the reactions (7) are related to the cross sections simply through the mean interatomic velocity $v=\sqrt{8kT/\pi\mu}$ by $k=\sigma v$ and they can be inferred from a rate equation approach.

In reaction (7a), usually known as energy transfer, the electronic energy of the A^* colliding atoms is totally transferred to only one of the two atoms that is excited to a higher level while the other atom is left in the ground state, as schematically shown in figure 6.

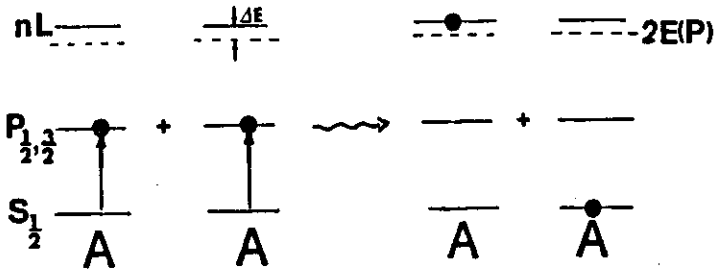

Figure 6. Sketch of the energy transfer in collisions between two excited atoms.

This process has been observed for all homonuclear alkali vapors [25] and the cross sections have been measured for many A^{**} final levels. An example of observed spectra is shown in figure 7 for the case of Rb(5P)/Rb(5P) collisions.

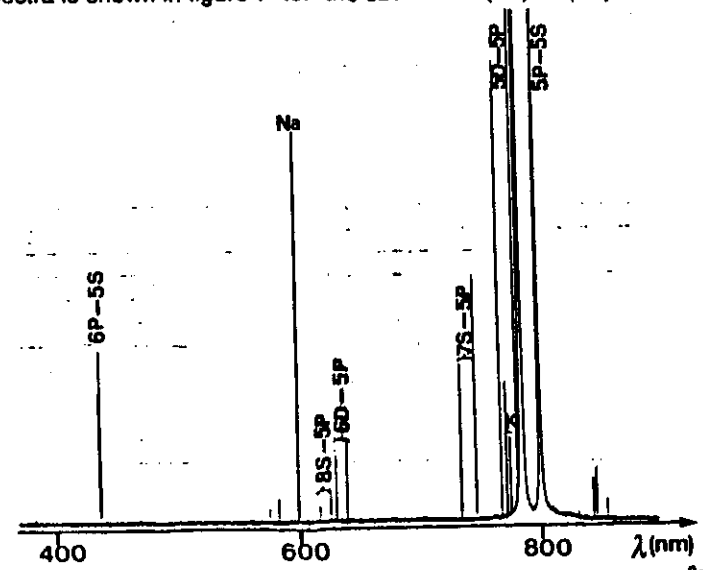

Figure 7. Fluorescence spectrum in the visible of rubidium vapor at T=200°C excited by a cw dye laser tuned to the $5S_{1/2}$--->$5P_{3/2}$ transition. Sodium and potassium resonance lines are present because of impurities in the cell.

In particular the sodium collisions Na(3P)/Na(3P) have been investigated with great accuracy [26,27,28], also taking into account the dependence on the J values of the 3P reactants [29]. A typical experiment consists in the excitation of sodium to the 3P state by a resonant laser and in the measurement of the fluorescence intensity from atoms in the 3P state and also in the nL states populated by the collisions. In the assumption that the energy transfer is the dominant process the evolution of the system is described by simple rate equations involving laser excitation, collisional transfer and spontaneous emission

$$N(nL) = k_{ET}(nL)N^2(3P) - \Sigma_{n'L'} A(nL,n'L')N(nL) + \Sigma_{n''L''}A(n''L'',nL)N(n''L'') \qquad (8)$$

where A(nL,n'L') is the spontaneous transition probability from level nL to the lower n'L' level. Solution of this equation at the steady-state and measurement of the ratio of the fluorescence intensities provide the rate constants $k_{ET}(nL) = \sigma_{ET}(nL)v$. The intensity of fluorescence lines from high levels nL is several orders of magnitude weaker than the resonance fluorescence 3P --->3S. However lines in the visible have been detected quite easily, while the detection of emissions in the infrared has required some more efforts [28]. As it is evident from equation (8), $k_{ET}(nL)$ depends upon the square of the excited atom density, a quantity that must be determined with high accuarcy in order to get correct values for $\sigma_{ET}(nL)$. Indeed the determination of excited atom density has been the major experimental problem, successfully solved by different approaches [26,27]. The order of magnitude of $\sigma_{ET}(nL)$ is $\sim 10^{-15} cm^2$ (precise values can be found for example in table 1A of reference [30]). This is a significant fraction of the kinetic geometrical cross section for two Na(3P) atoms, which is $\sim 10^{-14} cm^2$, showing the importance of reaction (7a). The measured cross sections are in good agreement with the values calculated from the nonadiabatic energy transfer in the molecular adiabatic potentials [28,31,32] and they are a good source of information on long range interactions.

In a mixture of two different alkali vapors the heteronuclear collisions between A^* and B^* excited atoms produce both A^{**} and B^{**} high-lying states

$$A^* + B^* \longrightarrow A^{**} + B \qquad (9)$$
$$\longrightarrow A + B^{**}$$

Tables for exit channels of processes (9) for all possible alkali pairs have been made [8] and cross section measurements have been reported for sodium/potassium energy transfer collisions [9,10]. Compared to homonuclear collisions there are two additional experimental difficulties: the relative atom density in a mixture can not be deduced simply from the temperature of the cell containing the saturated vapors and fluorescence originated from levels populated through A^*/B^* collisions must be discriminated from those produced by pure A^*/A^* and B^*/B^* collisions. Usually it is possible to prepare an amalgam of two different alkali metals such that at a certain temperature the two atom densities are comparable, while excited atom A^* and B^* densities are indipendently deduced from the effective radiative lifetimes measured in a resonance fluorescence experiment under pulsed excitation. To assure detection of processes due only to A^*/B^* collisions an intermodulation technique has been employed. The laser beams exciting A and B atoms are modulated at two different frequencies ω_A and ω_B and phase sensitive detection at the sum (or difference) frequency $\omega_A+\omega_B$ (or $\omega_A-\omega_B$) is used to monitored fluorescence emissions. A sketch of the apparatus is shown in figure 8. The cross sections so far measured for energy transfer in heteronuclear collisions are of the same order of magnitude as in pure alkali vapors. These values can be important for the knowledge of heteronuclear quasi-molecular potentials at internuclear distances for which few data are available.

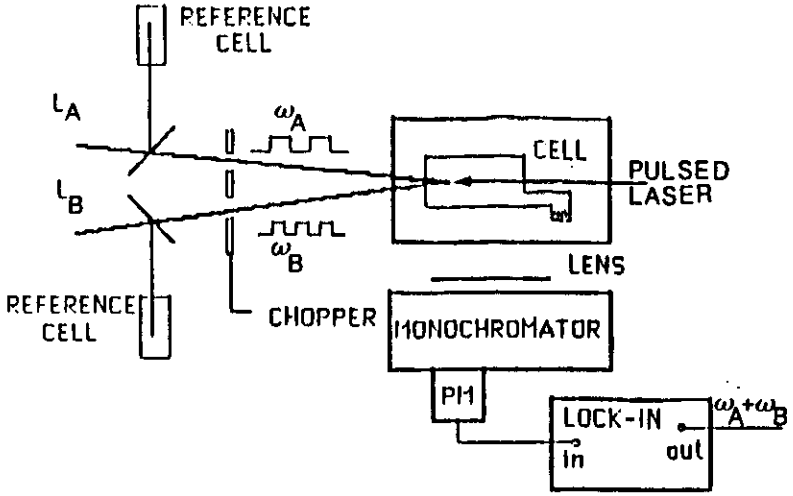

Figure 8. Sketch of the experimental apparatus for studies of heteronuclear collisions.

Reaction (7b) where two excited atoms combine in associative ionization to produce the molecular ion plus one electron ,is energetically possible for all alkalis but lithium for which the bottom of the ground state potential curve of Li_2^+ is too far from the sum energy of two Li(2P) atoms. Experiments investigating process (7b) have the same laser excitation apparatus as for energy transfer studies but different detection systems because ions, instead of fluorescence, have to be collected and identified. Rate equations similar to equation (8) can be written for the evolution of the molecular ion density $d[N(A_2^+)]/dt$ and measurements of the integrated A_2^+ signal provides the rate coefficients k_{AI} and cross sections σ_{AI}. Associative ionization in A^*/A^* collisions is the important reaction which provides the seed electrons (slow) initiating the mechanism of plasma formation. For sodium very precise measurements of σ_{AI} are available [33,34], also with velocity dependence [35] and polarization dependence [36]. These values are about two orders of magnitude smaller than typical σ_{ET}, indicating that the exit channel (7a) is the favoured one.

For the formation of the diatomic molecule in very excited electronic states, process (7c), to our knowledge, there are not measurements of k_{MF} and σ_{MF}, probably because of the complexity of the state manyfolds. Also it is not clear yet the exact mechanism of excited molecule formation from the incoming colliding A^*/A^* excited atoms since there has not been experimental evidence of direct energy transfer. However, the interest for this process is very strong because it provides a way to produce triplet molecular excited levels. As we said in the previous section of this work the ground triplet state of alkali diatomic molecules is mainly repulsive. This fact limits the possibility of investigation of triplet-triplet molecular transitions by absorption spectroscopy or laser induced fluorescence techniques. Through process (7c) triplet states are formed, (as well as singlet states), and they decay to the ground $^3\Sigma_u^+$ state originating diffuse bands [37,38.39]. Besides the intrinsic interest for spectroscopy of these states there is a specific important application as active medium in tunable laser sources, as suggested by Woerdman [39]. Optically pumped alkali dimer lasers, working on bound-bound transitions, are well known [40]; realization of optically pumped lasers working also on bound-free transitions (as in excimer lasers), would make the alkalis a unique laser medium covering almost in a continuous way the full spectrum from u.v. to near i.r..

3.2. Collisions involving Rydberg alkali atoms

Extension of interest from collisions between two atoms excited to the first P-resonance level to those involving atoms excited to higher levels has been immediate. Indeed collisions concerning highly excited atoms are very important processes in plasma physics and in astrophysics. Extensive researches have been dedicated to ion formation in collisions between one ground state atom and one Rydberg atom via the processes

$$\begin{aligned} A + A^{**} &\text{-----> } A^+ + A + e^- && \text{collisional ionization} \\ &\text{-----> } A_2^+ + e^- && \text{associative ionization} \\ &\text{-----> } A^+ + A^- && \text{ion-pair formation} \end{aligned} \qquad (10)$$

Investigations have been done again for all alkali vapors and the most extensive research is probably that on rubidium by Barbier and Cheret [41]. In addition to processes (10) we are also interested to certain reactive processes that lead to ion formation initiating from collisions where both reactants are highly excited atoms:

$$\begin{aligned} A^{**} + A^{**} &\text{-----> } A^+ + A + e^- \\ A^{**} + A^{**} &\text{-----> } A^+ + A^- \end{aligned} \qquad (11)$$

Here we will briefly report on some experiments on sodium [42,43], performed with the apparatus schematically shown in figure 9. Rydberg atoms Na^{**} (ns) or Na^{**}(nd) are produced by two-step laser excitation 3s-->3p-->nl in a stainless steel cell where the sodium density is measured by the technique of reference [5]. Two dye lasers (one yellow tuned to a D line and the other blue scanned over the 3p-->ns or 3p-->nd transitions) enter the cell in opposite directions and are pumped with the frequency doubled and tripled outputs of a Nd:YAG laser. The ions formed in the reaction region are electrostatically extracted from the cell, mass selected with a quadrupole mass filter and detected with a CuBe particle multiplier. Collection efficiency for positive and negative ions can be made nearly equal with a proper choice of the multiplier cathode potential and the overall voltage. The apparatus can be operated in two modes. In one mode both laser wavelengths are fixed and the mass spectrometer is scanned to identify the ions and to measure their relative abundances. Otherwise the mass spectrometer is set at a particular ion mass and the blue laser wavelength is scanned,

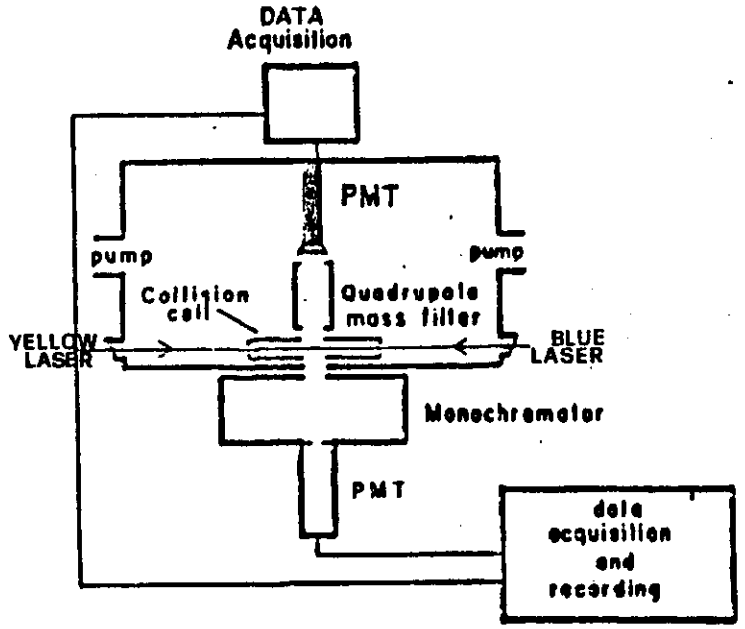

Figure 9. Schematic diagram of the apparatus for investigation of Rydberg/ground state and Rydberg/Rydberg collisions.

providing a spectrum that depends on the principal quantum number n. Further information can be obtained by studying the ion signals as function of atom density and power density of both dye lasers, even if for the yellow laser the range is limited by saturation of the 3s --> 3p transition. For sodium vapor containing Rydberg atoms Na^{**} the following mechanisms leading to ion formation have been studied

$$\begin{aligned} Na^{**} + Na &\text{-----> } Na^+ + Na + e^- && (12a) \\ Na^{**} + Na &\text{-----> } Na_2^+ + e^- && (12b) \\ Na^{**} + Na^{**} &\text{-----> } Na^+ + Na + e^- && (12c) \\ Na^{**} + h\nu_{bb} &\text{-----> } Na^+ + e^- && (12d) \end{aligned}$$

and their relative cross sections have been evaluated. The atom density N results a key parameter : at low N, ($< 10^{11} cm^{-3}$), heavy body collisions (12a), (12b), (12c)

are unimportant while photoionization by black body radiation (12d) dominates and it is responsible for virtually all observed Na^+. The Na^+ signal at $N=10^{11}cm^{-3}$ is observed to be nearly independent of the principal quantum number n over the range $18<n<30$ (see figure 2 of reference [43]). The total ion yield Q_{nl} can be written

$$Q_{nl} \propto R_{nl} N_{on} \tau_n \qquad (13)$$

with R_{nl} the black body photoionization rate, N_{on} the initial concentration of the Rydberg atoms and τ_n the lifetime of the Rydberg atom population. Since the dependences upon n of R_{nl} and N_{on} are proportional to $n^{-1.4}$ and n^{-3} respectively, to be consistent with the observed constancy of the Na^+ signal, the lifetime τ_n must vary approximately as $n^{4.4}$, in contrast with the n^3 dependence of a specific nl state. This dependence is very close to the $n^{4.5}$ dependence of a given n-state in hydrogen averaged over all angular momentum states. Thus, assuming valid the analogy between sodium and hydrogen atoms, we reach the important conclusion that the l-mixing rate by Na^{**}/Na collisions is so high that the state selectivity provided by the laser production of the Rydberg atoms is rapidly destroyed [43,44]. Using the information that total l-mixing is essentially complete prior to ionization it is possible to evaluate the cross sections for collisional ionization and associative ionization. Obviously these cross sections must be considered state specific only in the sense that the Na^{**} Rydberg atoms were initially prepared by the laser to a selected n-state, while the l-mixing has operated a redistribution of the excited state population over all angular momentum states. For $n=18$ Na^{**}/Na and Na^{**}/Na^{**} collisions contribute to the Na^+ signal with cross section $\sim 600 Å^2$ and about ten times geometric respectively, while Na^{**}/Na collisions produce Na_2^+ ions with a cross section $\sim 150 Å^2$. This last cross section however, decreases strongly, (see figure 4 of reference [43]), as $n^{-7.5}$ with increasing principal quantum number. This strong n-dependence is not surprising since the stabilization of the Na_2^+ product is given by the ejected Rydberg electron which interacts with the Na^++Na(3s) core complex. The strength of this interaction obviously depends upon the distance between the Rydberg electron and the core, therefore electrons in high n states and high l states are less reactive. Cross sections of processes (12) so measured can not be understood as intrinsic properties of state specific reactants but they are functions of other experimental parameters as the atom density N and the temperature T. T determines the black body radiation ionization process that can be controlled and virtually eliminated for example by cooling the cell. N determines the self l-mixing process that can not be eliminated because at atom densities low enough to preclude self l-mixing there would be essentially no heavy-body collisions.

Heteronuclear collisions involving Rydberg atoms can be studied as it has been done for A^*/B^* collisions, discussed in the previous paragraph. An example of the spectrum obtained for the reaction

$$Na^{**} + K \text{ -----> } K^+ + Na + e^- \qquad (14)$$

is shown in figure 10. However very little work has been done in this field and no cross section measurements have been reported so far.

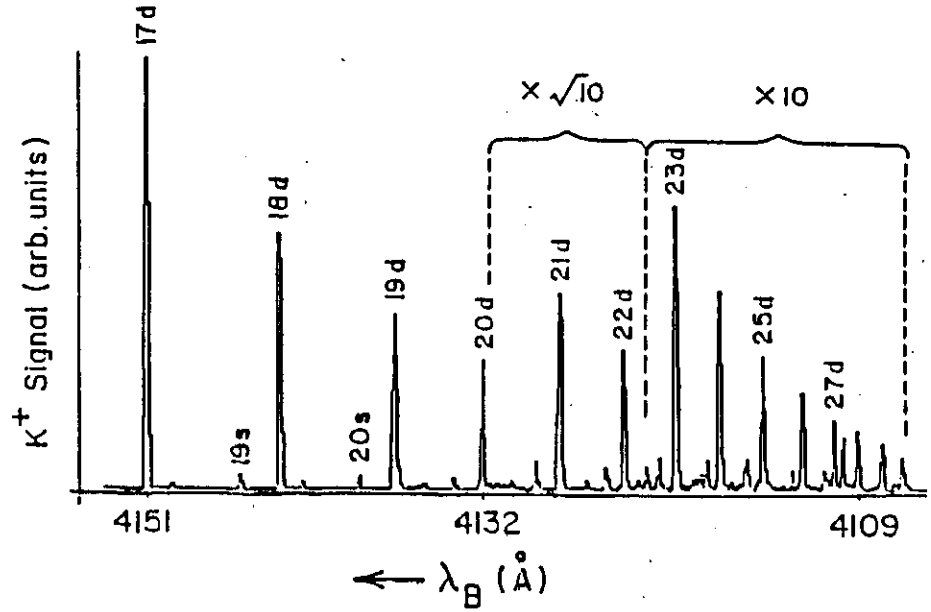

Figure 10. Spectrum of K^+ ions produced in collisions between sodium Rydberg atoms and potassium ground state atoms.

The same apparatus used to investigate processes (12) has allowed also the observation of negative ions. The experiment has been performed on sodium vapor and the only negative ion species observed was Na^- [46]. An obvious channel for Na^- production is

$$Na^{**} + Na \text{ -----> } Na^+ + Na^- \qquad (15)$$

which is an usual electron transfer process (for the energetic see for example figure 1 of reference [46]). However for high quantum numbers (n>18) the dependence of Na^- signal on laser power and on atom density clearly shows that the major source of negative ions are the Rydberg/Rydberg collisions

$$Na^{**} + Na^{**} \text{ -----> } Na^+ + Na^- \qquad (16)$$

If Na^+ and Na^- are formed in their ground state, reaction (16) is exothermic by ~5.5eV. Disposal of this huge energy amouny requires a complicate series of crossings with unknown energy curves from the entrance Na^{**}/Na^{**} channel to the Na^+/Na^- exit channel. Instead of this unlikely process two others alternative explanations have been advanced. An exit channel close to the Na^{**}/Na^{**} complex is provided by a product with Na^- formed in a doubly excited state with the outer electrons in correlated orbits (planetary negative ion). The third possible mechanism is radiative ion-pair process with formation of thermal Na^+ and Na^- plus simultaneous emission of a photon of ~5.5eV energy

$$Na^{**} + Na^{**} \text{ -----> } Na^+ + Na^- + h\nu \ (\sim 5.5eV) \qquad (17)$$

Photons of energy >5.5eV can be emitted because of the long range nature of the Coulomb force and process (17) is similar to radiative attachment in a Na^{**}/free electron collision. Whatever the exact mechanism leading to negative ion formation is, the large cross section for process (16) , that has been estimated of the order of $10^4 Å^2$ at n=20, suggestes that Rydberg/Rydberg interactions could be interesting sources for intensive negative ion beams, that are so imporatnt in plasma physics for neutral beam heating.

4. MECHANICAL ACTION OF RESONANCE LASER LIGHT ON ATOMIC MOTION

In this last section we will consider a phenomenon of atom-laser light interaction, based not on energy transfer, but on momentum transfer. In a medium optically excited by resonance laser light, the momentum transfer from absorbed photons to absorbing atoms is a well known phenomenon (radiation pressure) [47,48]. This effect has been proposed to control the velocity of the atoms for several applications like deflection [49-52] and stopping [53,54] of atomic beams, atom cooling [55-57] and isotope separation [58]. An extensive review on the effects of radiation pressure on free atoms is in reference [59]. For the observation of the resonance radiation pressure it is essential a collision free environment (as an atomic beam) because the photon momentum is very small compared to typical atomic momenta and collisions would mask the effect.

More recently it has been realized that light can affect also the motion of atoms immersed in a buffer gas. This new effect, known as LID (light induced drift), has been proposed by Gel'mukhanov and Shalagin [60] and observed for the first time by Antsygin et al. [61]. LID is not based on the direct transfer of the photon momentum to the atoms but to the combined effect of laser excitation and atomic collisions. The laser makes a velocity selected excitation of the atoms; in absence of buffer gas, i.e. in absence of velocity changing collisions, the drift of the excited atoms is compensated by the opposite drift of the ground state atoms and no macroscopic effect is observed. However, in presence of a buffer gas, i.e. in a strong collision environment, the mobility of excited and ground state atoms is different, resulting in a loss of symmetry in the Maxell velocity distribution and in a macroscopic drift of the atoms. This effect has been observed mainly in sodium vapor contained in a capillary cell with internal diameter of about the same size of the laser beam. Two spectacular demonstrations have been obtained for an optically thick vapor (optical piston) [62-64] and for an optically thin vapor (optical machine gun) [65,66].

LID is strongly affected by the collisions of the atoms with the cell walls because of the high atom-wall collision frequency in capillary cells having a radius comparable to the mean free path of the atoms. The adsorption of the atoms at the glass walls produces an enormous friction that can totally inhibit the drift. We have performed experiments [67,68] in absence of wall adsorption obtaining an impressive increase of the efficiency of LID. These experiments are also valuable for the study of the dynamics of the phenomenon and we have measured a drift velocity in good

agreement with the theoretical models [69]. The experiment consists in the excitation of sodium vapor with a single mode, actively stabilized dye laser, tuned to the D_2 line. Two pyrex capillary cells have been used, of the same shape and dimensions. One cell is without any coating so that the adsorption energy of the sodium atoms at the glass walls has the typical value of ~1eV; the internal surface of the second cell has been coated with a silane compound that reduces the adsorption energy by a factor ~10 and thus giving a wall frictionless regime. Similar results can be obtained also with other coating materials [65]. The LID effect is monitored by detecting the resonance fluorescence emitted by the excited atoms. To this purpose a movable optical fiber, connected to a photomultiplier, can sense all the length of the cell. The transient regime is studied by chopping the laser light and using a fast storage oscilloscope. The macroscopic effect of LID is shown in figure 11. The fluorescence

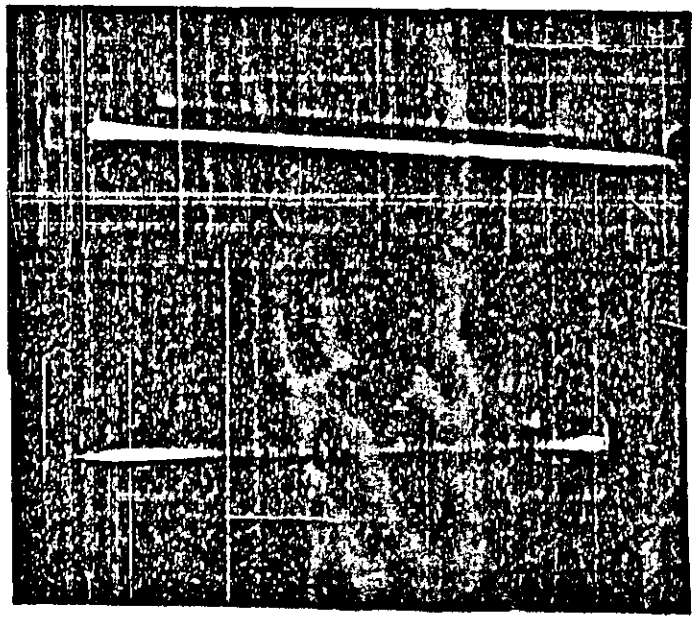

Figure 11. The uniform fluorescence inside the cell (a) is modified by the LID effect to a well localized spot (b).

signals can be studied as a function of i) the position of the fluorescence spot along the cell, ii) the laser detuning from the peak inside the absorption atomic line, iii) the intensity of the laser, and also as a function of other parameters like the temperature of the cell and the buffer gas pressure. All these features plus the time evolution, obtained when the laser was chopped, have given a clear picture of the LID phenomenon. Further experiments are in progress with broadband laser excitation and preliminary results have shown transient fluorescence signals about ten times faster than those obtained with single mode laser excitation [70], indicating more effective LID.

REFERENCES

1. Stwalley W.C. and Koch M.E., Optical Eng. 19, 71 (1980); Stwalley W.C., Koch M.E. and Verma K.K., in "Metal Bonding and Interactions in High Temperature Systems", Gole J.L. and Stwalley W.C. Eds., American Chemical Society Symposium Series 179, 397 (1982)
2. Nesmeyanov N., "Vapor Pressure of the Chemical Elements", (Elsevier, Amsterdam 1963)
3. see for example Ramsey N.F., "Molecular Beams" (Oxford 1956)
4. Vidal C.R. and Cooper J.J., J. Appl. Phys. 10, 3370 (1969)
5. Garver W.P., Pierce M.R. and Leventhal J.J., J. Chem. Phys. 77, 1201 (1982)
6. Huennekens J. and Gallagher A., Phys. Rev. A27 , 1851 (1983)
7. Wu. Z., Kitano M., Happer W., Hou M. and Daniels J., Appl. Opt. 25, 4483 (1986)
8. Cremoncini A., Abdullah S.A., Allegrini M., Gozzini S. and Moi L, Proc. Intern. Conf. LASERS' 85, (1986) pag. 98; Abdullah S.A., Allegrini M., Gozzini S. and Moi L., in "Photons and Continuum States of Atoms and Molecules", Rahman N.K., Guidotti C., and Allegrini M. Eds., Springer Proceedings in Physics 16, 214 (1987)
9. Allegrini M., Gozzini S. and Moi L., Proc. Intern. Conf. Laser Science II, in press
10. Gozzini S., Abdullah S.A., Allegrini M., Cremoncini A. and Moi L., Opt. Comm. 63, 97 (1987)
11. Bernheim R., "Optical Pumping. An Introduction" (W.A. Benjamin, New York 1965) pag. 64
12. see for example Cohen Tannoudji C. and Kastler A., Prog. in Opt. V, 3 (1966);

Happer W., Rev. Mod. Phys. 44, 169 (1972)
13. Kastler A., Acta Phys. Polon. 34, 693 (1968)
14. Alzetta G., Gozzini A. and Moi L., C.R. Acad. Sci. Paris 274, 39 (1972)
15. Moi L., Tesi Scuola di Perfezionamento, Universita' di Pisa 1978, unpublished
16. Allegrini M., Alzetta G., Bicchi P. and Gozzini S., 12th EGAS Conf. 1980, Summaries of Contributions n.5
17. Allegrini M., Bicchi P. and Gozzini S., J. Chem. Phys. 82, 457 (1985)
18. Allegrini M., Alzetta G., Bicchi P., Gozzini S. and Moi L., Ann. Phys. Fr. 10, 883 (1985)
19. Gozzini A., C.R. Acad. Sci. Paris 255, 1905 (1962); Proc. III Conf. Quantum Electronics, 1963 pag. 275
20. Silvera I.F. and Walraven J.T.M., Phys. Rev. Lett. 44, 164 (1980)
21. Cline R.W., Smith D.A., Greytak T.J. and Kleppner D., Phys. Rev. Lett. 45, 2117 (1980)
22. Lucatorto T.B. and McIlrath T.J., Phys. Rev. Lett. 37, 428 (1976)
23. Allegrini M., Alzetta G., Kopystynska A., Moi L. and Orriols G., Opt. Comm. 19, 96 (1976)
24. Allegrini M., Garver W.P., Kushawaha V.S. and Leventha J.J., Phys. Rev. A28, 199 (1983)
25. for reviews see: Lucatorto T.B. and McIlrath T.J., Appl. Opt. 19, 3948 (1980); Kopystynska A. and Moi L., Phys. Rep. 92, 135 (1982); Allegrini M., in "Fundamental Processes in Atomic Collisions Physics", Kleinpoppen H., Briggs J.S. and Lutz H.D. Eds. (Plenum Press 1985) pag. 460 Moi L., Acta Physica Polonica A69, 81 (1986)
26. Huennekens J. and Gallagher A., Phys. Rev. A27, 771 (1983)
27. Allegrini M., Bicchi P. and Moi L. , Phys. Rev. A28, 1338 (1983)
28. Allegrini M., Gabbanini C. and Moi L., Phys. Rev. A32, 2068 (1985)
29. Davidson S.A., Kelly J.F. and Gallagher A., Phys. Rev. A33, 3756 (1986)
30. Allegrini M., Gabbanini C. and Moi L., J. Physique 46, C1-61 (1985)
31. Kowalczyk P., Chem. Phys. Lett. 68, 203 (1079); Chem. Phys. Lett. 74, 80 (1980); J. Phys. B17, 817 (1984)
32. Henriet A., Masnou-Seeuws F. and LeSech C., Chem. Phys. Lett. 118, 507 (1985)
33. Bonanno R., Boulmer J. and Weiner J., Phys. Rev. A28, 604 (1983)
34. Huennekens J. and Gallagher A., Phys. Rev. A28, 1276 (1983)
35. Wang M-X., de Vries M.S., Keller J. and Weiner J.,Phys. Rev. A32, 681 (1985)
36. Jones D.M. and Dahler J.S., Phys. Rev. A31, 210 (1985); Wang M-X., de Vries M.S. and Weiner J., Phys. Rev. A33, 765 (1986); Phys. Rev. A34, 1869 (1986)
37. Allegrini M., Alzetta G., Kopystynska A., Moi L. and Orriols G., Opt. Comm. 22, 329 (1977)
38. Allegrini M., Gozzini S., Longo I., Savino P. and Bicchi P., Nuovo Cimento D1, 49 (1982)
39. Woerdman J.P., Opt. Comm. 26, 216 (1978)
40. for tables of alkali dimer optically pumped lasers see for example: Bahns J.T., Rajaei-Rizi A.R., Verma K.K., Orth F.B. and Stwalley W.C., Proc. Intern. Conf. LASERS' 82, (1983), pag. 713
41. Barbier L. and Cheret M., J. Phys. B20, 1229 (1987) and references therein
42. Burkhardt C.E., Garver W.P., Kushawaha V.S. and Leventhal J.J., Phys. Rev. A30, 653 (1984)
43. Burkhardt C.E., Corey R.L., Garver W.P., Leventhal J.J., Allegrini M. and Moi L., Phys. Rev. A34, 80 (1986)
44. Allegrini M., Gozzini S., Moi L., Burkhardt C.E., Ciocca M., Corey R.L., Garver W.P. and Leventhal J.J., Laser Spectroscopy VII, Hansch T.W. and Shen Y.R. Eds., (Srpinger Verlag, 1985) pag. 90
45. Bethe H.A. and Salpeter E.E., "The Quantum Mechanics of One and Two Electron Atoms", (Academic, New York 1957)
46. Ciocca M., Allegrini M., Arimondo E., Burkhardt C.E., Garver W.P. and Leventhal J.J., Phys. Rev. Lett. 58, 704 (1986)
47. Frisch O.R., Z. Phys. 86, 42 (1933)
48. Ashkin A., Phys. Rev. Lett. 24, 156 (1970); Bjorkholm J.E., Ashkin A. and Pearson D.B., Appl. Phys. Lett. 27, 534 (1975); Bjorkholm J.E., Freeman R.R., Ashkin A. and Pearson D.B., Phys. Rev. Lett. 41, 1361 (1978)
49. Ashkin A., Phys. Rev. Lett. 25, 1321 (1970); Phys. Rev. Lett. 40, 729 (1978)
50. Schieder R., Walther H. and Woste L., Opt. Comm. 5, 337 (1972)
51. Pique J.L. and Vialle J.L., Opt. Comm. 5, 402 (1972); Jaquinot P., Liberman S., Pique J.L. and Pinard J., Opt. Comm. 8, 163 (1973)
52. Arimondo E., Lew H. and Oka T., Phys. Rev. Lett. 43, 753 (1979); Gould P.L., Ruff G.A., and Pritchard D.E., Phys. Rev Lett. 56, 827 (1986)
53. Prodan J., Migdall A., Phillips W.D., So I. and Dalibard H., Phys. Rev. Lett. 54, 992

(1985)
54. Ertmer E., Blatt Z., Hall J.L. and Zhu M., Phys. Rev. Lett. 54, 996 (1985)
55. Hansch W. and Shawlow A.L., Opt. Comm. 13, 68 (1975)
56. Balykin V.I., Letokhov V.S., Minogin V.G. and Zueva T.V., Appl. Phys. B35, 149 (1984)
57. Chu S., Bjorkholm J.E. Ashkin A. and Cable A., Phys. Rev. Lett. 57, 314 (1986)
58. Bernhardt A.F., Duerre D.E., Simpson J.R. and Wood L.L., Appl. Phys. Lett. 25, 617 (1974)
59. Letokhov V.S. and Minogin V.G., Phys. Rep. 73, 1 (1981)
60. Gel'mukhanov F. Kh. and Shalagin A.M., Sov. Phys. JETP Lett. 29, 711 (1979); Sov. Phys. JETP 51, 839 (1980)
61. Antsygin V.D., Atutov S.N., Gel'mukhanov F.Kh., Telegin G.G. and Shalagin A.M., Sov. Phys. Lett. 30, 243 (1979)
62. Werij H.G.C., Woerdman J.P., Beenakker J.J.M. and Kuscer I., Phys. Rev. Lett. 52, 2237 (1984)
63. Werij H.G.C., Haverkort J.E.M. and Woerdman J.P., Phys. Rev. A33, 3270 (1986)
64. Hamel W.A., Streater A.D. and Woerdman J.P., Opt. Comm. 63, 32 (1987)
65. Atutov S.N., Lesjak St., Podjachev S.P. and Shalagin A.M., Opt. Comm. 60, 41 (1986)
66. Werij H.G.C., Haverkort J.E.M., Planken P.C.M., Eliel E.R., Woerdman J.P., Atutov S.N., Chapovsky P.L. and Gel'muchanov, Phys. Rev. Lett., in press
67. Moi L., Allegrini M., Gozzini S., Mariotti E. and Xu J.H., Proc. Intern. Conf. LASERS'86, in press
68. Xu J.H., Allegrini M., Gozzini S., Mariotti E. and Moi L., Opt. Comm. 63, 43 (1987)
69. Nienhuis G., Phys. Rep. 138, 151 (1986); Phys. Rev. A31, 1636 (1986)
70. Xu J.H., Gozzini S., Allegrini M., Alzetta G., Mariotti E. and Moi L., Laser Spectroscopy VIII, 1987 in press